ParB spreading on DNA requires cytidine triphosphate *in vitro*

Adam S. B. Jalal[1], Ngat T. Tran[1], and Tung B. K. Le[1*]

[1]Department of Molecular Microbiology

John Innes Centre, Norwich, NR4 7UH, United Kingdom

[*]For correspondence: tung.le@jic.ac.uk

ABSTRACT

In all living organisms, it is essential to transmit genetic information faithfully to the next generation. The SMC-ParAB-*parS* system is widely employed for chromosome segregation in bacteria. A DNA-binding protein ParB nucleates on *parS* sites and must associate with neighboring DNA, a process known as spreading, to enable efficient chromosome segregation. Despite its importance, how the initial few ParB molecules nucleating at *parS* sites recruit hundreds of further ParB to spread is not fully understood. Here, we reconstitute a *parS*-dependent ParB spreading event using purified proteins from *Caulobacter crescentus* and show that CTP is required for spreading. We further show that ParB spreading requires a closed DNA substrate, and a DNA-binding transcriptional regulator can act as a roadblock to attenuate spreading unidirectionally *in vitro*. Our biochemical reconstitutions recapitulate many observed *in vivo* properties of ParB and opens up avenues to investigate the interactions between ParB-*parS* with ParA and SMC.

INTRODUCTION

Faithful chromosome segregation is essential in all domains of life if daughter cells are each to inherit the full set of genetic information. The SMC-ParAB-*parS* complex is widely employed for chromosome segregation in bacteria [1–13]. The centromere *parS* is the first DNA locus to be segregated following chromosome replication [8,9,14,15]. ParB specifically nucleates on *parS* before spreading outwards to the flanking DNA and bridges/cages DNA together to form a nucleoprotein network *in vivo* [16–23]. This nucleoprotein complex recruits SMC to disentangle and organize replicated DNA [3,11,13,24,25]. ParB-*parS* also interacts with an ATPase ParA to power the segregation of replicated chromosomes [26–30]. Engineered strains harboring a nucleation-competent but spreading-defective mutant of *parB* are either unviable [10] or have elevated number of anucleate cells [4,7,8,15,31–34]. Despite the importance of spreading for proper chromosome segregation, the mechanism by which a few *parS*-bound ParB can recruit hundreds more ParB molecules to the vicinity of *parS* to assemble a high molecular-weight nucleoprotein complex is not fully understood.

Since the first report in 1995 [35], ParB spreading has been observed *in vivo* by chromatin immunoprecipitation in multiple bacterial species [12,15–17,19,36]. The nucleation of ParB on *parS* has also been demonstrated *in vitro* [4,10,16,17,20,37–39], however *parS*-dependent ParB spreading has resisted biochemical reconstitution [17–19,40,41]. Unsuccessful attempts to reconstitute spreading *in vitro* suggests that additional factors might be missing. Recently, works by Soh et al (2019) and Osorio-Valeriano et al (2019) on *Bacillus subtilis* and *Myxococcus xanthus* ParB, respectively, showed that ParB binds and hydrolyzes cytidine triphosphate (CTP) to cytidine diphosphate (CDP), and that CTP modulates the binding affinity of ParB to *parS* [42,43]. A co-crystal structure of *Bacillus* ParB with CDP and that of a *Myxococcus* ParB-like protein (PadC) with CTP showed CTP binding promotes a new dimerization interface between N-terminal domains of ParB subunits [42,43]. Crucially, Soh et al (2019) showed by single-molecule imaging and cross-linking assays that *Bacillus* ParB, in the presence of CTP, forms a self-loading protein clamp at *parS* and slides away to spread to neighboring DNA [43]. While reproducing a key result from Easter and Gober (2002) that showed *Caulobacter crescentus* ParA-ATP dissociated pre-bound ParB from *parS* [44], we found that CTP could also modulate the nucleation of *Caulobacter* ParB on *parS*. Personal communication with Stephan Gruber and the recent work by Osorio-Valeriano et al (2019) and Soh et al (2019) encouraged us to take steps further to investigate the role of CTP for ParB spreading in *Caulobacter crescentus*.

Here, we reconstitute a *parS*-dependent ParB spreading on DNA in real-time, using a label-free purified protein from *Caulobacter crescentus*. Consistent with pioneering works by Soh et al (2019) and Osorio-Valeriano et al (2019), we confirm that CTP regulates ParB-DNA interaction. We further provide evidence that the accumulation of *Caulobacter* ParB requires a closed DNA substrate, and that a DNA-binding transcription factor, TetR, can act as a roadblock to attenuate ParB accumulation unidirectionally *in vitro*. Our real-time and label-free reconstitution has successfully recapitulated many well-known aspects of ParB behaviors *in vivo* and might open up avenues to investigate further the roles of the ParB-*parS* nucleoprotein complex in ensuring faithful chromosome segregation.

RESULTS

CTP reduces the nucleation of *Caulobacter* ParB on *parS*

Easter and Gober (2002) reported that ATP-bound *Caulobacter* ParA dissociated ParB from *parS* [44], however the authors did not control for the effect of ATP alone on ParB-*parS* binding. NTPs are highly negatively charged and could have affected protein-DNA interactions by binding non-specifically to the often positively charged DNA-binding domain. To determine if ATP or other NTP alone affects ParB-*parS* interaction, we attached a linear 20-bp biotinylated *parS* DNA to a streptavidin-coated probe to measure the bio-layer interference (BLI) (Figure 1A). BLI assay monitors wavelength shifts (responses) resulting from changes in the optical thickness of the probe surface during association or dissociation of the analyte (see Materials and Methods). We

monitored in real-time interactions between immobilized *parS* DNA and purified *Caulobacter* ParB or a premix of ParB + NTP (Figure 1B). Consistent with previous reports [12,45], *Caulobacter* ParB bound site-specifically to *parS* but not to non-cognate DNA (Figure 1-figure supplement 1). In the presence of ATP, GTP, or UTP, we observed a small reduction in ParB-*parS* binding at steady state regardless of whether Mg^{2+} was included in binding buffer or not (Figure 1B and Figure 1-figure supplement 2), suggesting that *Caulobacter* ParB is slightly sensitive to highly negatively charged compounds or to counter-ions (Na^{+}) in NTP solutions. However, we noted that CTP had a pronounced effect on ParB-*parS* interaction, specifically in the presence of Mg^{2+} (Figure 1B and Figure1-figure supplement 2). An increasing concentration of CTP (but not CMP or CDP) gradually reduced the binding of ParB to *parS* (Figure 1-figure supplement 3). In contrast, neither CTP nor other NTPs affected the binding of another protein-DNA pair, for example, the well-characterized TetR-*tetO* interaction [46] (Figure 1C). On closer inspection, we noted that ParB + CTP slowly dissociated from *parS* even before the probe was returned to a protein-free buffer (a gradual downward slope between 30th and 150th sec, Figure 1B), suggesting that CTP facilitated ParB removal from a 20-bp *parS* DNA. To investigate further, we monitored the dissociation rates of pre-bound CTP-free ParB-*parS* complexes after probes were returned to a protein-free buffer with or without CTP, we found ParB dissociating ~seven times faster in buffer with CTP than in buffer only solution (Figure 1D). Given the short length of a 20-bp *parS* DNA duplex that has only sufficient room for nucleation, our results suggest that CTP might decrease ParB nucleation on *parS* or liberates pre-bound ParB from *parS* site.

CTP facilitates ParB accumulation on a closed DNA substrate

Next, we investigated the effect of CTP on ParB-DNA interaction by employing a longer 169-bp *parS*-containing DNA fragment that has been labeled at both 5' ends with biotin (Figure 2A). Immobilizing a dual biotin-labeled DNA on a streptavidin-coated BLI probe created a DNA substrate where both ends were blocked (a closed DNA) [47] (Figure 2-figure supplement 1). We monitored the interactions between immobilized DNA and purified *Caulobacter* ParB in the presence or absence of NTP. In the absence of NTP, we observed the usual nucleation event on *parS* with 1 μM ParB protein (Figure 2A). We noted that the BLI signal was not as high as with a 20-bp *parS* probe (Figure 2A) due to a less efficient immobilization of a longer DNA fragment on the BLI probe. Premixing ATP, GTP, or UTP with ParB did not change the sensorgrams markedly (Figure 2A). However, the addition of CTP significantly increased the response by ~12 fold (Figure 2A and Figure 2-figure supplement 2A), suggesting that more ParB associated with a 169-bp *parS* probe at steady state than by nucleation at *parS* alone. We observed that DNA-bound ParB was salt sensitive and dissociated readily to the solution when the BLI probe was returned to a low-salt protein-free buffer without CTP (Figure 2A, dissociation phase). However, the dissociation of pre-bound ParB-CTP from DNA was slowed down by ~fivefold if the probe was returned to a buffer supplemented with CTP (Figure 2-figure supplement 2B). The effect on the BLI response was not seen if Mg^{2+} was omitted (Figure 2-figure supplement 2C), neither did we observe an equivalent increase in response when a 169-bp dual biotin-labeled DNA containing a scrambled *parS* was employed instead (Figure 2A). Furthermore, we observed that a nucleation-competent but spreading-defective *Caulobacter* ParB (R104A) [12] mutant did not respond to the addition of CTP to the same extent as ParB (WT) (Figure 2B). Our results suggest that CTP is required for the increase in *parS*-dependent ParB accumulation *in vitro*. Lastly, we performed BLI experiments for eight additional chromosomal ParB proteins from a diverse set of bacterial species and consistently observed the specific effect of CTP on enhancing ParB association with a closed DNA *in vitro* (Figure 2-figure supplement 3). It is most likely that ParB-CTP interaction with DNA is conserved among ParB orthologs.

To independently verify the BLI data, we performed an *in vitro* pull-down of purified His-tagged *Caulobacter* ParB (Figure 2C). Streptavidin-coated paramagnetic beads were incubated with 2.8-kb dual biotin-labeled DNA fragments containing either *parS* or scrambled *parS* sites. Again, a dual biotin-labeled DNA formed a closed substrate on the surface of the beads. DNA-coated beads were incubated with purified *Caulobacter* ParB either in the presence or absence of NTP before

being pulled down magnetically. Pulled-down ParB was released from beads and their protein level was analyzed by an α-His_6 immunoblot (Figure 2C). We found ~13-15 fold more pulled-down ParB when CTP was included (Figure 2C). No enrichment was observed when scrambled *parS*-coated beads were used, confirming that the extensive *in vitro* association of ParB with DNA is dependent on *parS* (Figure 2C). Also, consistent with the BLI experiments, no further enrichment of ParB was seen when ATP, GTP or UTP was included (Figure 2C). Furthermore, a ParB (R104A) variant was not enriched in our pull-down assay regardless of whether CTP was present or not (Figure 2C). Altogether, our results suggest that a *parS*-dependent accumulation of ParB on a closed DNA substrate requires CTP.

A closed DNA substrate is required for an increased ParB association with DNA

Next, we investigated whether a DNA substrate with a free end (an open DNA) can also support ParB accumulation *in vitro*. The 169-bp dual biotin-labeled DNA was designed with unique *Bam*HI and *Eco*RI recognition sites flanking the *parS* site (Figure 3A). To generate an open end on DNA, we immerged the DNA-coated probes in buffers contained either *Bam*HI or *Eco*RI (Figure 3A-C and Figure 3-figure supplement 1). Before restriction enzyme digestion, we again observed an enhanced ParB association with a closed DNA substrate in the presence of CTP (Figure 3A). After digestion by either *Bam*HI or *Eco*RI, the inclusion of CTP had no effect on the BLI response, indicating that ParB did not accumulate on an open DNA substrate *in vitro* (Figure 3B-C). Our conclusion was further supported by results from an experiment in which we added *Bam*HI after ParB + CTP and a closed DNA substrate were preincubated together for 120 sec (Figure 3-figure supplement 2). Here, in the presence of *Bam*HI, ParB binding to DNA reduced gradually over 30 min, while it was unaffected if heat-inactivated *Bam*HI was employed instead (Figure 3-figure supplement 2). Lastly, consistent with BLI experiments, our pull-down assay also showed that ParB-CTP failed to accumulate when a 2.8-kb dual biotin-labeled DNA was linearized by *Hind*III digestion (Figure 3D).

Next, we wondered if a tight protein-DNA binding could cap the open end of DNA, thereby mimicking a closed DNA substrate and restoring ParB accumulation. To investigate this possibility, we constructed a 170-bp dual biotin-labeled DNA fragment that contains a single *parS* site, a *tetO* operator, and flanking restriction enzyme recognition sites for *Eco*RI and *Bam*HI (Figure 4A). With this closed DNA substrate, we observed an enhanced ParB association with DNA in the presence of CTP (Figure 4A). Again, we generated a free DNA end via restriction enzyme digestion. Consistent with previous experiments with a restricted 169-bp DNA probe, the addition of ParB + CTP had no effect on the BLI response (Figure 4B). However, it can be partially rescued by incubating a *Bam*HI-restricted DNA probe with a premix of ParB + CTP + TetR (Figure 4B). We reason that TetR binding at *tetO* capped the open DNA end, essentially generated a closed DNA substrate. Our conclusion was further supported by results from an experiment in which a premix of ParB + CTP + TetR was tested against an *Eco*RI-restricted DNA instead (Figure 4C). Here, we did not observe an enhanced association of ParB with DNA even when TetR was included, most likely because of a persistent open DNA end that could not be blocked by TetR-*tetO* binding (Figure 4C). Finally, we observed that the TetR could attenuate ParB-CTP accumulation on a closed DNA substrate (magenta line vs. orange line, Figure 4A). This blocking effect is specific to TetR-*tetO* binding since the addition of anhydrotetracycline (ahTc), a negative effector of TetR [46], allowed ParB-CTP to regain its accumulation on DNA (Figure 4-figure supplement 1). Overall, the ability of a DNA-bound TetR to act as a roadblock *in vitro* is consistent with previous ChIP-seq data that showed DNA-binding proteins or RNA polymerases could block or attenuate ParB spreading unidirectionally *in vivo* [16,17,20,36].

***parS* DNA increases the CTP binding and hydrolysis rate of *Caulobacter* ParB**

Recently, *Myxococcus* and *Bacillus* ParB were shown to bind and hydrolyze CTP [42,43]. Our *in vitro* results so far also hint at CTP binding directly to *Caulobacter* ParB. By employing a membrane-spotting assay (DRaCALA), we showed that *Caulobacter* ParB binds to radiolabeled CTP in the presence of *parS* DNA (Figure 5A). An excess of unlabeled CTP, but no other NTPs, could

compete with radioactive CTP for binding to *Caulobacter* ParB (Figure 5B), suggesting that *Caulobacter* ParB does not bind other NTPs. The CTP binding of ParB was reduced when a non-cognate DNA site (*NBS*) [48] was used instead of *parS* (Figure 5A). We also failed to detect CTP binding in our DRaCALA assay or by isothermal titration calorimetry when DNA was omitted. Nevertheless, we robustly detected CTP hydrolysis to CDP and inorganic phosphate when *Caulobacter* ParB and CTP were included, albeit at a very low rate of ~0.4 CTP molecules per ParB per hour (Figure 5C). A background level of inorganic phosphate was observed when *Caulobacter* ParB was incubated with ATP, GTP, or UTP (Figure 5C). Crucially, the addition of a 22-bp *parS* DNA, but not a non-cognate 22-bp *NBS* DNA, increased CTP turnover rate sevenfold to ~3 CTP molecules per ParB per hour (Figure 5C). Lastly, the CTP hydrolysis was reduced to the background in the nucleation-competent but spreading-defective ParB (R104A) variant (Figure 5C). Altogether, our data suggest that *parS* DNA stimulates *Caulobacter* ParB to bind and hydrolyze CTP.

ParB accumulation on DNA is unstable in the presence of a non-hydrolyzable analog CTPγS

Next, we investigated the role of CTP hydrolysis by following ParB-*parS* interaction in the presence of a non-hydrolyzable analog CTPγS (Figure 6A and Figure 6-figure supplement 1). ParB was preincubated with CTP or CTPγS for 1 to 60 min before binding to a 169-bp closed *parS* DNA substrate (Figure 6A). We observed that *Caulobacter* ParB could accumulate on DNA in the presence of CTPγS, but in contrast to when CTP was employed, a longer preincubation time between ParB and CTPγS gradually reduced ParB accumulation on DNA (Figure 6A). Our results suggest the possibility that CTPγS, in the absence of *parS* DNA, converts apo-ParB in solution to a nucleation-incompetent form over time. Our observation is reminiscent of a time-course experiment in which CTPγS efficiently promoted the engagement between N-terminal domains of *Bacillus* ParB in the absence of *parS* DNA [43]. The engagement of N-terminal domains was shown to convert *Bacillus* ParB from an open to a closed protein clamp [43]. If not already bound on DNA, the closed form of ParB presumably cannot nucleate/load onto *parS* due to its now inaccessible DNA-binding domain [43]. We wondered if CTPγS also catalyzed the N-domain engagement in *Caulobacter* ParB in the absence of *parS* DNA. To investigate this possibility, we employed site-specific cross-linking of a purified *Caulobacter* ParB (Q35C C297S) variant by a sulfhydryl-to-sulfhydryl crosslinker bismaleimidoethane (BMOE) (Figure 6B). A lone cysteine residue on the native ParB was first mutated to serine to create a cysteine-less ParB (C297S) variant, then a glutamine to cysteine mutation was engineered at position 35 at the N-terminal domain to create ParB (Q35C C297S). Both ParB (C297S) and ParB (Q35C C297S) were competent at spreading in the presence of CTP (Figure 6-figure supplement 2A). The cross-linking of ParB (Q35C C297S) was also enhanced by CTP and CTPγS but not by other NTPs, consistent with the specific role of CTP in ParB spreading (Figure 6-figure supplement 2B). We performed a time-course cross-linking of ParB (Q35C C297S) + CTP or CTPγS in the absence of *parS* DNA (Figure 6B). As shown in Figure 6B, CTPγS was twice as efficient as CTP in promoting the cross-linked form between N-terminal domains of *Caulobacter* ParB. The rapid increase in the nucleation-incompetent closed form of *Caulobacter* ParB might explain the overall reduction in accumulation overtime when ParB was preincubated with CTPγS (Figure 6A).

To further investigate the effect of CTPγS on ParB spreading on a longer time scale, we extended the association phase between 169-bp *parS* DNA and a freshly prepared premix of ParB + CTP or CTPγS from 120 sec to 60 min (Figure 6C). In the presence of CTP, the reaction reached steady state after 120 sec and remained stable for the duration of the association phase (Figure 6C). However, in the presence of CTPγS, ParB accumulation rapidly reached the maximal level after 200 sec, then declined slowly over 60 min. We suggest that DNA-bound ParB-CTPγS complexes gradually dissociated from DNA into solution (possibly via a transient clamp opening or CTPγS leaving its weak binding pocket rather than by hydrolysis) but were not replenished by a new cycle of nucleation-spreading-dissociation because over time most ParB-CTPγS in solution was in a nucleation-incompetent closed form. Taken together, we suggest that CTP hydrolysis is not

required for *parS*-bound ParB to escape the nucleation site to spread, but possibly contributes to maintaining the stability of spreading by recycling ParB.

DISCUSSION

In this work, we report that a small molecule (CTP) is required to enable *Caulobacter* ParB proteins (as well as eight other chromosomal ParB proteins, Figure 2-figure supplement 3) to spread *in vitro*. Recently, Soh *et al* (2019) observed that F-plasmid and P1-plasmid ParB proteins also bind and hydrolyze CTP [43]. Hence, it is most likely that the effect of CTP on ParB spreading is universal among plasmid and chromosomal ParB orthologs. A classical mutant whose arginine-rich patch (G^{101}ERRxR) has been mutated to alanine e.g. ParB (R104A) [8] was not responsive to CTP, suggesting that CTP is bound to the N-terminal domain of *Caulobacter* ParB. Indeed, Soh *et al* (2019) reported a co-crystal structure that showed CDP binding to the arginine-rich patch at the N-terminal domain of *Bacillus* ParB (CTP was hydrolyzed to CDP during crystallization) [43]. Osorio-Valeriano *et al* (2019) also showed a similar binding pocket of CTP at the N-terminal domain of *Myxococcus* ParB by hydrogen-deuterium exchange mass spectrometry [42]. Intriguingly, a co-crystal structure of a *Helicobacter pylori* ParB-*parS* complex, together with the *in vitro* magnetic-tweezer and single-molecule TIRF microscopy-based experiments with *Bacillus* ParB showed that the N-terminal domain can oligomerize to bridge DNA together without the need of an additional ligand [18,19,37,40]. There might be two different modes of action of ParB on DNA: one for bridging DNA together (that does not require CTP) and another for the lateral spreading of ParB on DNA (that requires CTP). Investigating the relative contribution of these two different modes of action to chromosome segregation *in vivo* is an important challenge for the future.

The requirement of a DNA substrate with blocked ends for ParB accumulation *in vitro* is suggestive of a lateral ParB diffusion along the DNA i.e. ParB can escape by running off a free DNA end (Figure 7). Inside cells, the spreading and bridging/caging of ParB have been inferred from the compact foci of fluorescently labeled ParB [4,15,20,49–53], presumably resulting from the concentration of fluorescent signal to a defined location in the cytoplasm. Nucleation-competent but spreading-defective ParB mutants formed no or very diffusive foci *in vivo* [19,54]. Recently, it has been observed that an artificially engineered double-strand break ~8 kb away from *parS* did not cause a dissolution of ParB foci in *Caulobacter* cells [55]. This result seemingly contradicted our findings that *Caulobacter* ParB spreading *in vitro* requires a closed DNA. However, we reason that the abundant DNA-bound transcription factors and RNA polymerases *in vivo* act as roadblocks to minimize ParB runoff. This barricading effect has been recapitulated in our experiments with TetR, a tight DNA-binding transcriptional regulator (Figure 4).

Our results so far suggest three distinct stages of *Caulobacter* ParB-DNA interactions *in vitro*:

Stage 1: ParB nucleates on *parS* (Figure 7A). Results from experiments in Figure 1 indicate that CTP modulates ParB nucleation on a *parS* site. Soh *et al* (2019) reported that CTP-bound ParB could form a closed protein clamp even in the absence of *parS* DNA, albeit not energetically favorable [43]. The DNA-binding domain of a closed ParB clamp would be inaccessible to DNA, especially to a closed DNA substrate. It might be that only apo-ParB or a transiently formed CDP-bound ParB (from CTP hydrolysis) are able to nucleate on *parS* (Figure 7A). Supporting this interpretation, preincubation of *Caulobacter* ParB with a non-hydrolyzable analog CTPγS promoted efficiently the cross-linked form of ParB and subsequently reduced ParB nucleation and spreading on DNA (Figure 6). Initially, we were surprised by a weak CTP binding of *Bacillus*, *Caulobacter*, and *Myxococcus* ParBs [42,43], however, this might be advantageous for the cells as a fraction of intracellular apo-ParB will remain to nucleate on *parS*.

Stage 2: Nucleated ParB escapes from *parS* (Figure 7B-C). We showed that *Caulobacter* ParB-*parS* complex binds CTP, and this facilitates ParB dissociation from *parS* (Figure 1D). It was reported that the DNA-binding domain in *Bacillus* ParB-CDP co-crystal structure is incompatible with *parS* binding [43] and this might enable ParB to escape from a high-affinity nucleation site to non-specific flanking DNA. Our observation of a low BLI response with an open DNA (Figure 3 and

Figure 4) implies that ParB proteins dissociate off the free end well before the next ParB escapes from the *parS* nucleation site. We suggest that the transition from a *parS*-bound ParB to a spreading ParB might be the rate-limiting step.

Stage 3: ParB spreads or diffuses to non-specific DNA flanking *parS*. Our observation that *Caulobacter* ParB did not accumulate on an open DNA suggests that *Caulobacter* ParB diffuses laterally along the DNA. Similarly, cross-linking experiments on *Bacillus* ParB [43] proposed that the ParB-CTP complex forms a sliding clamp that moves along the DNA [43]. From our experiments with CTPγS (Figure 6) and consistent with Soh et al (2019), we suggest that the diffusive *Caulobacter* ParB along the DNA is CTP bound. The low CTP hydrolysis rate of *Caulobacter* ParB (~3 CTP molecules per ParB per hour) while ParB spreading could be observed by BLI within minutes also lends support to the interpretation that the diffusive spreading form of *Caulobacter* ParB is most likely CTP-bound (Figure 7B-C). For *Bacillus* and *Caulobacter* ParB, CTP hydrolysis is not required for ParB to escape from the nucleation site [43]. *Caulobacter* ParB could still spread on a DNA when incubated with a non-hydrolyzable CTPγS (Figure 6), even though spreading, at least *in vitro*, was less stable over time in comparison to when CTP was employed (Figure 6C). As suggested for *Bacillus* ParB [43] and supported by our results with *Caulobacter* ParB, CTP hydrolysis might contribute to ParB recycling instead. It is possible that ParB recycling *in vivo* is achieved via several routes: (i) CTP dissociation from its weak binding pocket, (ii) CTP hydrolysis, (iii) a possible enhanced CTP dissociation/hydrolysis via collisions with DNA-bound roadblocks, or (iv) a transient clamp opening even when ParB is CTP bound. Additional work is required to investigate the dynamics of ParB clamp opening/closing, and whether both CTP molecules on opposite subunits of a ParB dimer are concertedly hydrolyzed/dissociated for ParB to escape from the chromosome or a heterodimer state of ParB with a single CTP bound exists *in vivo*.

FINAL PERSPECTIVES

In this work, we showed the enhancing effect of CTP on *Caulobacter* ParB accumulation on DNA and further demonstrated that ParB spreading requires a closed DNA substrate and that a DNA-binding transcriptional regulator can act as a roadblock to attenuate spreading unidirectionally *in vitro*. Our real-time and label-free reconstitution of ParB spreading has successfully recapitulated many well-known aspects of ParB behaviors and is consistent with pioneering works by Soh et al (2019) and Osorio-Valeriano et al (2019). Beyond the biological significance of the findings, our label-free approaches to biochemical reconstitution obviate the often time-consuming and challenging task of site-specifically labeling proteins with fluorophores/chemical crosslinkers without affecting the function of proteins. Here, we have demonstrated the medium-throughput capability of our methodology by investigating the effect of CTP on the spreading of eight additional chromosomal ParB proteins. The ease and medium-throughput manner of our methodology is likely to facilitate future works by the community. Important areas of research in the future are to investigate (i) the effect of ParB-CTP spreading on the supercoiling state of the DNA and vice versa, and (ii) how ParA and SMC interact with ParB-CTP *in vivo* to organize and faithfully segregate replicated chromosomes to each daughter cell.

ACKNOWLEDGEMENTS

This study was funded by the Royal Society University Research Fellowship (UF140053), BBSRC grant (BB/P018165/1 and BBS/E/J/000PR9791), and Royal Society Research Grant (RG150448) (to T.B.K.L). We thank Dr. Wilma Ross (Department of Bacteriology, University of Wisconsin, Madison) for advice on DRaCALA assays, and Dr. Clare Stevenson (Biophysical Platform, John Innes Centre) for assistance in biophysical techniques. We thank Dr. César López Pastrana (Faculty of Physics, Technical University of Munich) for valuable feedback on the manuscript, and Dr. Stephan Gruber and Dr. Martin Thanbichler for sharing reagents and data.

MATERIALS AND METHODS

Key Resources Table

Reagent type (species) or resource	Designation	Source or reference	Identifiers	Additional information
strain, strain background (*Escherichia coli*)	Rosetta (DE3)	Merck	Cat# 70954	Electro-competent cells
recombinant DNA reagent	See supplementary file 1	This paper	See supplementary file 1	
sequence-based reagent	See supplementary file 1	This paper	See supplementary file 1	
antibody	Anti-6xHis tag antibody (HRP) (Rabbit polyclonal)	Abcam	Cat# ab1187	Western blot (1:5,000)
commercial assay or kit	EnzChek Phosphate Assay Kit	ThermoFisher	Cat# E6646	
commercial assay or kit	Gibson Assembly Master Mix	NEB	Cat# E2611S	
commercial assay or kit	Gateway BP Clonase II enzyme mix	ThermoFisher	Cat# 11789020	
commercial assay or kit	Dip-and-Read Streptavidin (SA) biosensors	Molecular Devices	Cat# 18-5019	
commercial assay or kit	HisTrap High Performance column	GE Healthcare	Cat# GE17524801	
commercial assay or kit	HiTrap Heparin High Performance column	GE Healthcare	Cat# GE17040601	
commercial assay or kit	HiLoad 16/600 Superdex 75pg column	GE Healthcare	Cat# GE28989333	
commercial	Dynabeads MyOne	ThermoFisher	Cat# 65001	

assay or kit	Streptavidin C1			
commercial assay or kit	Amersham Protran supported Western blotting membranes, nitrocellulose	GE Healthcare	Cat# GE10600016	pore size 0.45 µm, for DRaCALA assay
Recombinant protein	*Bam*HI-HF	NEB	Cat# R3136S	20,000 units/mL
Recombinant protein	*Bam*HI	NEB	Cat# R0136S	20,000 units/mL
Recombinant protein	*Eco*RI-HF	NEB	Cat# R3101S	20,000 units/mL
Recombinant protein	*Hind*III-HF	NEB	Cat# R3104S	20,000 units/mL
Recombinant protein	Exonuclease VII	NEB	Cat# M0379S	10,000 units/mL
Recombinant protein	Exonuclease T7	NEB	Cat# M0263S	10,000 units/mL
chemical compound, drug	Benzonase nuclease	Sigma-Aldrich	Cat# E1014	
chemical compound, drug	NTP	ThermoFisher	Cat# R0481	100 mM solution
chemical compound, drug	CTPγS	Jena Bioscience	Custom synthesis	A gift from S. Gruber and custom synthesis (purity ≥ 96%)
chemical compound, drug	CMP-PCP	Jena Bioscience	Cat# NU-254	
chemical compound, drug	P^{32}-α-CTP	Perkin Elmer	Cat# BLU008H250UC	3000 Ci/mmol, 10 mCi/ml, 250 µCi
chemical compound, drug	Anhydrotetracycline hydrochloride (ahTc)	Abcam	Cat# ab145350	Dissolved in ethanol

chemical compound, drug	Bismaleimidoethane (BMOE)	ThermoFisher	Cat# 22323	Dissolved in DMSO
software, algorithm	BLItz Pro	Molecular Devices	https://www.moleculardevices.com/	Version 1.2
software, algorithm	R	R Foundation for Statistical Computing	RRID: SCR_001905	Version 3.2.4
software, algorithm	Image Studio Lite	LI-COR Biosciences	https://www.licor.com/bio/image-studio-lite/	Version 5.2
software, algorithm	Excel 2016	Microsoft	https://products.office.com	

Protein overexpression and purification

Full-length *Caulobacter* ParB (WT) and ParB (R104A) were purified as described previously [12]. Briefly, pET21b::ParB-His_6 (WT or R104A) was introduced into *E. coli* Rosetta (DE3) competent cells (Merck). A 10 mL overnight culture was used to inoculate 4 L of LB medium + carbenicillin + chloramphenicol. Cells were grown at 37°C with shaking at 250 rpm to an OD_{600} of 0.4. The culture was then left to cool to 4°C before isopropyl-β-D-thiogalactopyranoside (IPTG) was added to a final concentration of 1 mM. The culture was shaken for 3 hours at 30°C before cells were harvested by centrifugation.

Pelleted cells were resuspended in a buffer containing 100 mM Tris-HCl pH 8.0, 300 mM NaCl, 10 mM Imidazole, 5% (v/v) glycerol, 1 µL of Benzonase nuclease (Sigma Aldrich), 1 mg of lysozyme (Sigma Aldrich), and an EDTA-free protease inhibitor tablet (Roche). The pelleted cells were then lyzed by sonication. The cell debris was removed via centrifugation at 28,000 g for 30 min, and the supernatant was filtered through a 0.45 µm sterile filter (Sartorius Stedim). The protein was then loaded into a 1-mL HisTrap column (GE Healthcare) that had been equilibrated with buffer A [100 mM Tris-HCl pH 8.0, 300 mM NaCl, 10 mM Imidazole, and 5% glycerol]. Protein was eluted from the column using an increasing (10 mM to 500 mM) imidazole gradient in the same buffer. ParB-containing fractions were pooled and diluted to a conductivity of 16 mS/cm before being loaded onto a 1-mL Heparin HP column (GE Healthcare) that had been equilibrated with 100 mM Tris-HCl pH 8.0, 25 mM NaCl, and 5% glycerol. Protein was eluted from the Heparin column using an increasing (25 mM to 1 M NaCl) salt gradient in the same buffer. ParB that was used for EnzChek Phosphate assay and DRaCALA was further polished via a gel-filtration column. To do so, purified ParB was concentrated by centrifugation in an Amicon Ultra-15 3-kDa cut-off spin filters (Merck) before being loaded into a Superdex 75 gel filtration column (GE Healthcare). The gel filtration column was pre-equilibrated with 100 mM Tris-HCl pH 8.0, 250 mM NaCl, and 1 mM $MgCl_2$.

C-terminally His-tagged TetR (class B, from Tn10) were expressed from *E. coli* Rosetta DE3) harboring a pET21b::TetR-His_6 plasmid (Supplementary file 1). TetR-His_6 were purified via a one-step Ni-affinity column using the exact buffers as employed for the purification of *Caulobacter* ParB-His_6.

C-terminally His-tagged ParB (C297S) and ParB (Q35C C297S) were expressed from *E. coli* Rosetta (DE3) harboring a pET21b::ParB-His_6 (C297S) or (Q35C C297S) plasmid (Supplementary file 1). ParB-His_6 (C297S) and (Q35C C297S) were purified via a one-step Ni-affinity column using the exact buffers as employed for the purification of *Caulobacter* ParB-His_6. ParB (Q35C C297S)

stock solution was supplemented with TCEP (1 mM final concentration) before being flash-frozen in liquid nitrogen.

N-terminally His-tagged MBP-tagged ParB (orthologous proteins from various bacterial species) were expressed from *E. coli* Rosetta (DE3) harboring pET-His-MBP-TEV-DEST::ParB plasmids (Table S1). His_6-MBP-ParB proteins were purified via a one-step Ni-affinity column as described previously [56].

Different batches of proteins were purified by A.S.B.J and N.T.T, and are consistent in all assays used in this work. Both biological (new sample preparations from a fresh stock aliquot) and technical (same sample preparation) replicates were performed for assays described in this study.

Construction of pET21b::ParB-His_6 (C297S and Q35C C297S)

DNA containing the codon-optimized coding sequence of ParB (C297S or Q35C C297S) was chemically synthesized (gBlocks dsDNA fragments, IDT). These gBlocks fragments and a *Nde*I-*Hind*III-digested pET21b backbone were assembled using a 2x Gibson master mix (NEB). Two and a half µL of each fragment at equimolar concentration was added to 5 µL 2x Gibson master mix (NEB), and the mixture was incubated at 50°C for 60 min. Five µL was used to transform chemically competent *E. coli* DH5α cells. Gibson assembly was possible due to a 23-bp sequence shared between the *Nde*I-*Hind*III-cut pET21b backbone and the gBlocks fragments. These 23-bp regions were incorporated during the synthesis of gBlocks fragments. The resulting plasmids were sequence verified by Sanger sequencing (Eurofins, Germany).

Construction of pET21b::TetR-His_6

DNA containing the coding sequence of TetR (class B, from Tn10) was chemically synthesized (gBlocks dsDNA fragments, IDT). This gBlocks fragment and a *Nde*I-*Hind*III-digested pET21b backbone were assembled together using a 2x Gibson master mix (NEB). Gibson assembly was possible due to a 23-bp sequence shared between the *Nde*I-*Hind*III-cut pET21b backbone and the gBlocks fragment. These 23-bp regions were incorporated during the synthesis of gBlocks fragments. The resulting plasmids were sequence verified by Sanger sequencing (Eurofins, Germany).

Construction of pENTR::ParB orthologs

The coding sequences of ParB orthologs were chemically synthesized (gBlocks dsDNA fragments, IDT) and cloned into pENTR-D-TOPO backbone (Invitrogen) by Gibson assembly (NEB). The resulting plasmids were sequence verified by Sanger sequencing (Eurofins, Germany).

Construction of pET-His-MBP-TEV-DEST::ParB orthologs

The *parB* genes were recombined into a Gateway-compatible destination vector pET-His-MBP-TEV-DEST [56] via an LR recombination reaction (ThermoFisher). For LR recombination reactions: 1 µL of purified pENTR::*parB* (~100 ng/µL) was incubated with 1 µL of the destination vector pET-His-MBP-TEV-DEST (~100 ng/µL), 1 µL of LR Clonase II enzyme mix, and 2 µL of water in a total volume of 5 µL.

Construction of DNA substrates for BLI assays

All DNA constructs (Supplementary file 1) were designed in VectorNTI (Thermo Fisher) and were chemically synthesized (gBlocks dsDNA fragments, IDT). All linear DNA constructs were designed with M13F and M13R homologous regions at each end. To generate a dual biotin-labeled DNA substrate, PCR reactions were performed using a 2x GoTaq PCR master mix (Promega), biotin-labeled M13F and biotin-labeled M13R primers, and gBlocks fragments as template. PCR products were resolved by electrophoresis and gel purified.

Measurement of protein-DNA interaction by bio-layer interferometry (BLI)

Bio-layer interferometry experiments were conducted using a BLItz system equipped with Dip-and-Read Streptavidin (SA) Biosensors (Molecular Devices). BLItz monitors wavelength shifts (nm) resulting from changes in the optical thickness of the sensor surface during association or dissociation of the analyte. All BLI experiments were performed at 22°C. The streptavidin biosensor was hydrated in a low-salt binding buffer [100 mM Tris-HCl pH 8.0, 100 mM NaCl, 1 mM $MgCl_2$, and 0.005% Tween 20] for at least 10 min before each experiment. Biotinylated double-stranded DNA (dsDNA) was immobilized onto the surface of the SA biosensor through a cycle of Baseline (30 sec), Association (120 sec), and Dissociation (120 sec). Briefly, the tip of the biosensor was dipped into a binding buffer for 30 sec to establish the baseline, then to 1 μM biotinylated dsDNA for 120 sec, and finally to a low salt binding buffer for 120 sec to allow for dissociation.

After the immobilization of DNA on the sensor, association reactions were monitored at 1 μM dimer concentration of ParB (with or without 1 μM TetR or NTPs at various concentrations) for 120 sec or 60 min (Figure 6A). At the end of each binding step, the sensor was transferred into a protein-free binding buffer to follow the dissociation kinetics for 120 sec. The sensor can be recycled by dipping in a high-salt buffer [100 mM Tris-HCl pH 8.0, 1000 mM NaCl, 1 mM $MgCl_2$, and 0.005% Tween 20] for 5 min to remove bound ParB.

For experiments where a closed DNA was cleaved to generate a free DNA end, DNA-coated tips were dipped into 300 μL of cutting solution [266 μL of water, 30 μL of 10x CutSmart buffer (NEB), and 4 μL of *Eco*RI-HF or *Bam*HI-HF restriction enzyme (20,000 units/mL)] for 30 min at 37°C.

For experiments described in Figure 1-figure supplement 2, $MgCl_2$ was omitted from all binding and protein storage buffers.

For experiments described in Figure 3-figure supplement 2, bio-layer interferometry assays were performed using 1x NEB 3.1 buffer [100 mM NaCl, 50 mM Tris-HCl pH 7.9, 10 mM $MgCl_2$, 100 μg/ml BSA] instead of the low-salt binding buffer [100 mM NaCl, 10 mM Tris-HCl pH 8.0, 1 mM $MgCl_2$, 0.005% Tween20]. After incubating 1 μM ParB and 1 mM CTP with a 169 bp *parS*-coated probe for 120 sec, 4 μL of *Bam*HI (20,000 units/mL) or heat-inactivated *Bam*HI was added to a 300 μL reaction to start digesting bound DNA. The reaction was monitored for an additional 30 min. *Bam*HI was inactivated by heat at 65°C for 30 min.

For experiments described in Figure 4-figure supplement 1, 3 μM of anhydrotetracycline (ahTc) was used to remove bound TetR from DNA. After incubating 1 μM ParB and 1 mM CTP ± 1 μM TetR with a 170-bp *parS*-coated probe for 120 sec, ahTc (dissolved in ethanol) or ethanol alone was added to a 300 μL reaction to the final concentration of 3 μM or 0.01%, respectively. The reaction was monitored for an additional 120 sec.

All sensorgrams recorded during BLI experiments were analyzed using the BLItz analysis software (BLItz Pro version 1.2, Molecular Devices) and replotted in R for presentation. Each experiment was triplicated, the standard deviation of triplicated sensorgrams is less than ten percent, and a representative sensorgram was presented in each figure.

To verify that dual biotin-labeled DNA fragments formed a closed substrate on the surface of the BLI probe, we performed a double digestion with Exonuclease T7 and Exonuclease VII (NEB) (Figure 2-figure supplement 1). DNA-coated tips were dipped into 300 μL of cutting solution [266 μL of water, 30 μL of 10x RE buffer 4 (NEB), 2 μL of exonuclease T7 (10,000 units/mL) and 2 μL of exonuclease VII (10,000 units/mL)] for 30 min at 25°C. Tips were then cut off from the plastic adaptor (Figure 2-figure supplement 1) and immerged into a 1x GoTaq PCR master mix [25 μL water, 25 μL 2x GoTaq master mix, 0.5 μL of 100 μM M13F oligo, and 0.5 μL of 100 μM M13R oligo]. Ten cycles of PCR were performed, and the PCR products were resolved on 2% agarose gels (Figure 2-figure supplement 1).

NTP (stock concentration: 100 mM) used in BLI assays was purchased from ThermoFisher. CTPγS (stock concentration: 90 mM) was a generous gift from Stephan Gruber and Young-Min Soh. CTPγS was also custom-synthesized and re-purified to 96% purity (Jena Bioscience). Another non-hydrolyzable analog CMP-PCP (Jena Bioscience) was unsuitable for our assays as *Caulobacter* ParB does not bind CMP-PCP (Figure 6-figure supplement 1).

Construction of DNA substrates for pull-down assays

A 260-bp DNA fragment containing *Caulobacter parS* sites (genomic position: 4034789-4035048) [12] or scrambled *parS* sites were chemically synthesized (gBlocks fragments, IDT). These DNA fragments were subsequently 5' phosphorylated using T4 PNK enzyme (NEB), then cloned into a *Sma*I-cut pUC19 using T4 DNA ligase (NEB). The two resulting plasmids are pUC19::260bp-*parS* and pUC19::260bp-scrambled *parS* (Supplementary file 1). These plasmids were sequence verified by Sanger sequencing (Eurofins, Germany). To generate dual biotin-labeled DNA substrates, we performed PCR using a pair of biotinylated primers: around_pUC19_F and around_pUC19_R, and either pUC19::260bp-*parS* or pUC19::260bp-scrambled *parS* as a template. Phusion DNA polymerase (NEB) was employed for this round-the-horn PCR reaction. The resulting ~2.8-kb linear DNA fragments were gel-purified and eluted in 50 µL of autoclaved distilled water.

Pull-down assays

Paramagnetic MyOne Streptavidin C1 Dyna beads (ThermoFisher) were used for pull-down assays. Thirty µL of beads were washed twice in 500 µL of high-salt wash buffer [100 mM Tris-HCl pH 8.0, 1 M NaCl, 1 mM $MgCl_2$, and 0.005% Tween 20] and once in 100 µL binding buffer [100 mM Tris-HCl pH 8.0, 100 mM NaCl, 1 mM $MgCl_2$, and 0.005% Tween 20] by repeating a cycle of resuspension and pull-down by magnetic attraction. Five µL of ~50 nM dual biotin-labeled DNA substrate was incubated with 30 µL of beads in 100 µL binding buffer for 30 min at room temperature. The reaction was occasionally mixed by pipetting up and down several times. Afterward, DNA-coated beads were washed once in 500 µL high-salt buffer [100 mM Tris-HCl pH 8.0, 1000 mM NaCl, 1 mM $MgCl_2$, and 0.005% Tween 20] and once in 500 µL of binding buffer. Finally, DNA-coated beads were resuspended in 300 µL of binding buffer. Ninety-six µL of the resuspended beads were used for each pull-down assay. Four µL of *Caulobacter* ParB-His_6 (WT) or (R104A) (stock concentration: 25 µM) were added to 96 µL of suspended beads. NTPs were either omitted or added to the suspended beads to the final concentration of 1 mM. The mixture was pipetted up and down several times and was left to incubate at room temperature for 5 min. Beads were then pulled down magnetically and unwanted supernatant discarded. DNA-coated beads (now with bound protein) were then washed once with 500 µL of binding buffer and once with 100 µL of the same buffer. The unwanted supernatant was discarded, and the left-over beads were resuspended in 30 µL of 1x SDS-PAGE sample buffer. Each experiment was triplicated, and a representative immunoblot was presented.

Immunoblot analysis

For immunoblot analysis, magnetic beads were resuspended directly in 1x SDS sample buffer, then heated to 42°C for 15 min before loading to 12% Novex Tris-Glycine SDS-PAGE gels (ThermoFisher). The eluted protein was resolved by electrophoresis at 150 V for 60 min. Resolved proteins were transferred to polyvinylidene fluoride membranes using the Trans-Blot Turbo Transfer System (BioRad) and probed with 1:5,000 dilution of α-His_6 HRP-conjugated antibody (Abcam). Blots were imaged and analyzed using an Amersham Imager 600 (GE Healthcare) and Image Studio Lite version 5.2 (LI-COR Biosciences). The band intensities were quantified for lanes 5 and 6 (Figure 2C), and the range of fold difference between replicates was reported.

Differential radial capillary action of ligand assay (DRaCALA) or membrane-spotting assay

Purified *Caulobacter* ParB-His_6 or TetR-His_6 (final concentration: 25 μM) were incubated with 5 nM radiolabeled P^{32}-α-CTP (Perkin Elmer), 30 μM of unlabeled cold CTP (Thermo Fisher), 1.5 μM of 22-bp *parS* or *NBS* DNA duplex in the reaction buffer [100 mM Tris pH 8.0, 100 mM NaCl, and 10 mM $MgCl_2$] for 5 minutes at room temperature. For the NTP competition assay, the mixture was further supplemented with 500 μM of either unlabeled cold CTP, ATP, GTP, or UTP. Four μL of samples were spotted slowly onto a dry nitrocellulose membrane and air-dried. The nitrocellulose membrane was wrapped in cling film before being exposed to a phosphor screen (GE Healthcare) for two minutes. Each DRaCALA assay was triplicated, and a representative autoradiograph was shown.

DNA preparation for EnzCheck Phosphate assay and DRaCALA

A 22-bp palindromic single-stranded DNA fragment (*parS*: GGATGTTTCACGTGAAACA TCC or *NBS*: GGATATTTCCCGGGAAATATCC) [100 μM in 1 mM Tris-HCl pH 8.0, 5 mM NaCl buffer] was heated at 98°C for 5 min before being left to cool down to room temperature overnight to form 50 μM double-stranded *parS* or *NBS* DNA. The sequences of *parS* and *NBS* are underlined.

Measurement of NTPase activity by EnzCheck Phosphate assay

NTP hydrolysis was monitored using an EnzCheck Phosphate Assay Kit (Thermo Fisher). Samples (100 μL) containing a reaction buffer supplemented with 1 mM of NTP and 1 μM ParB (WT or R104A) were assayed in a Biotek EON plate reader at 25°C for 15 hours with readings every minute. The reaction buffer (1 mL) typically contained: 740 μL Ultrapure water, 50 μL 20x customized reaction buffer [100 mM Tris pH 8.0, 2 M NaCl, and 20 mM $MgCl_2$], 200 μL MESG substrate solution, and 10 μL purine nucleoside phosphorylase (1 unit). Reactions with buffer only, buffer + protein only or buffer + NTP only were also included as controls. The plates were shaken at 280 rpm continuously for 15 hours at 25°C. The inorganic phosphate standard curve was also constructed according to the manual. Each assay was triplicated. The results were analyzed using R and the NTPase rates were calculated using a linear regression fitting in R.

***In vitro* crosslinking using a sulfhydryl-to-sulfhydryl crosslinker bismaleimidoethane (BMOE)**

A 50 μL mixture of 10 μM ParB (C297S) or (C297S Q35C) ± 1 mM NTP ± 0.5 μM *parS* dsDNA (22 bp) was assembled in a reaction buffer [10 mM Tris-HCl pH 7.4, 100 mM NaCl, and 1 mM $MgCl_2$] and incubated for 15 min (Figure 6-figure supplement 2B) or for 1, 5, 10, 15, and 30 min (Figure 6B) at room temperature. BMOE (1 mM final concentration from a 20 mM stock solution) was then added, and the reaction was quickly mixed by three pulses of vortexing. SDS-PAGE sample buffer containing 23 mM β-mercaptoethanol was then added immediately to quench the crosslinking reaction. Samples were heated to 50°C for 15 min before being loaded on 12% TruPAGE Tris-Glycine Precast gels (Sigma Aldrich). Each assay was triplicated. Gels were stained with InstantBlue solution (Expedeon) and band intensity was quantified using Image Studio Lite version 5.2 (LI-COR Biosciences). The crosslinked fractions were averaged, and their standard deviations calculated in Excel.

REFERENCES

1. Donczew, M. *et al.* ParA and ParB coordinate chromosome segregation with cell elongation and division during Streptomyces sporulation. *Open Biology* **6**, 150263 (2016).
2. Fogel, M. A. & Waldor, M. K. A dynamic, mitotic-like mechanism for bacterial chromosome segregation. *Genes Dev.* **20**, 3269–3282 (2006).
3. Gruber, S. & Errington, J. Recruitment of condensin to replication origin regions by ParB/SpoOJ promotes chromosome segregation in B. subtilis. *Cell* **137**, 685–96 (2009).
4. Harms, A., Treuner-Lange, A., Schumacher, D. & Sogaard-Andersen, L. Tracking of chromosome and replisome dynamics in Myxococcus xanthus reveals a novel chromosome arrangement. *PLoS Genet* **9**, e1003802 (2013).

5. Ireton, K., Gunther, N. W. & Grossman, A. D. spo0J is required for normal chromosome segregation as well as the initiation of sporulation in Bacillus subtilis. *J. Bacteriol.* **176**, 5320–5329 (1994).
6. Jakimowicz, D., Chater, K. & Zakrzewska-Czerwi´nska, J. The ParB protein of Streptomyces coelicolor A3(2) recognizes a cluster of parS sequences within the origin-proximal region of the linear chromosome. *Molecular Microbiology* **45**, 1365–1377 (2002).
7. Kawalek, A., Bartosik, A. A., Glabski, K. & Jagura-Burdzy, G. Pseudomonas aeruginosa partitioning protein ParB acts as a nucleoid-associated protein binding to multiple copies of a parS-related motif. *Nucleic Acids Res.* **46**, 4592–4606 (2018).
8. Lin, D. C.-H. & Grossman, A. D. Identification and Characterization of a Bacterial Chromosome Partitioning Site. *Cell* **92**, 675–685 (1998).
9. Livny, J., Yamaichi, Y. & Waldor, M. K. Distribution of Centromere-Like parS Sites in Bacteria: Insights from Comparative Genomics. *J. Bacteriol.* **189**, 8693–8703 (2007).
10. Mohl, D. A., Easter, J. & Gober, J. W. The chromosome partitioning protein, ParB, is required for cytokinesis in Caulobacter crescentus. *Mol. Microbiol.* **42**, 741–755 (2001).
11. Sullivan, N. L., Marquis, K. A. & Rudner, D. Z. Recruitment of SMC by ParB-parS organizes the origin region and promotes efficient chromosome segregation. *Cell* **137**, 697–707 (2009).
12. Tran, N. T. *et al.* Permissive zones for the centromere-binding protein ParB on the Caulobacter crescentus chromosome. *Nucleic Acids Res* **46**, 1196–1209 (2018).
13. Wang, X., Brandão, H. B., Le, T. B. K., Laub, M. T. & Rudner, D. Z. Bacillus subtilis SMC complexes juxtapose chromosome arms as they travel from origin to terminus. *Science* **355**, 524–527 (2017).
14. Toro, E., Hong, S.-H., McAdams, H. H. & Shapiro, L. Caulobacter requires a dedicated mechanism to initiate chromosome segregation. *PNAS* **105**, 15435–15440 (2008).
15. Lagage, V., Boccard, F. & Vallet-Gely, I. Regional Control of Chromosome Segregation in Pseudomonas aeruginosa. *PLOS Genetics* **12**, e1006428 (2016).
16. Breier, A. M. & Grossman, A. D. Whole-genome analysis of the chromosome partitioning and sporulation protein Spo0J (ParB) reveals spreading and origin-distal sites on the Bacillus subtilis chromosome. *Molecular Microbiology* **64**, 703–718 (2007).
17. Murray, H., Ferreira, H. & Errington, J. The bacterial chromosome segregation protein Spo0J spreads along DNA from parS nucleation sites. *Molecular Microbiology* **61**, 1352–1361 (2006).
18. Taylor, J. A. *et al.* Specific and non-specific interactions of ParB with DNA: implications for chromosome segregation. *Nucleic Acids Res* **43**, 719–731 (2015).
19. Graham, T. G. W. *et al.* ParB spreading requires DNA bridging. *Genes Dev.* **28**, 1228–1238 (2014).
20. Sanchez, A. *et al.* Stochastic Self-Assembly of ParB Proteins Builds the Bacterial DNA Segregation Apparatus. *Cell Syst.* **1**, 163–173 (2015).
21. Debaugny, R. E. *et al.* A conserved mechanism drives partition complex assembly on bacterial chromosomes and plasmids. *Mol. Syst. Biol.* **14**, e8516 (2018).
22. Broedersz, C. P. *et al.* Condensation and localization of the partitioning protein ParB on the bacterial chromosome. *PNAS* **111**, 8809–8814 (2014).
23. Funnell, B. E. ParB Partition Proteins: Complex Formation and Spreading at Bacterial and Plasmid Centromeres. *Front Mol Biosci* **3**, 44 (2016).
24. Tran, N. T., Laub, M. T. & Le, T. B. K. SMC Progressively Aligns Chromosomal Arms in Caulobacter crescentus but Is Antagonized by Convergent Transcription. *Cell Rep* **20**, 2057–2071 (2017).
25. Minnen, A., Attaiech, L., Thon, M., Gruber, S. & Veening, J.-W. SMC is recruited to oriC by ParB and promotes chromosome segregation in Streptococcus pneumoniae. *Mol. Microbiol.* **81**, 676–688 (2011).
26. Lim, H. C. *et al.* Evidence for a DNA-relay mechanism in ParABS-mediated chromosome segregation. *Elife* **3**, e02758 (2014).
27. Vecchiarelli, A. G., Neuman, K. C. & Mizuuchi, K. A propagating ATPase gradient drives transport of surface-confined cellular cargo. *Proc. Natl. Acad. Sci. U.S.A.* **111**, 4880–4885 (2014).

28. Vecchiarelli, A. G., Mizuuchi, K. & Funnell, B. E. Surfing biological surfaces: exploiting the nucleoid for partition and transport in bacteria. *Molecular Microbiology* **86**, 513–523 (2012).
29. Hwang, L. C. *et al.* ParA-mediated plasmid partition driven by protein pattern self-organization. *The EMBO Journal* **32**, 1238–1249 (2013).
30. Leonard, T. A., Butler, P. J. & Löwe, J. Bacterial chromosome segregation: structure and DNA binding of the Soj dimer--a conserved biological switch. *EMBO J.* **24**, 270–282 (2005).
31. Jecz, P., Bartosik, A. A., Glabski, K. & Jagura-Burdzy, G. A single parS sequence from the cluster of four sites closest to oriC is necessary and sufficient for proper chromosome segregation in Pseudomonas aeruginosa. *PLoS ONE* **10**, e0120867 (2015).
32. Attaiech, L., Minnen, A., Kjos, M., Gruber, S. & Veening, J.-W. The ParB-parS Chromosome Segregation System Modulates Competence Development in Streptococcus pneumoniae. *mBio* **6**, e00662-15 (2015).
33. Yu, W., Herbert, S., Graumann, P. L. & Götz, F. Contribution of SMC (Structural Maintenance of Chromosomes) and SpoIIIE to Chromosome Segregation in Staphylococci. *J Bacteriol* **192**, 4067–4073 (2010).
34. Lee, P. S. & Grossman, A. D. The chromosome partitioning proteins Soj (ParA) and Spo0J (ParB) contribute to accurate chromosome partitioning, separation of replicated sister origins, and regulation of replication initiation in Bacillus subtilis. *Mol. Microbiol.* **60**, 853–869 (2006).
35. Lynch, A. S. & Wang, J. C. SopB protein-mediated silencing of genes linked to the sopC locus of Escherichia coli F plasmid. *PNAS* **92**, 1896–1900 (1995).
36. Rodionov, O., Lobocka, M. & Yarmolinsky, M. Silencing of genes flanking the P1 plasmid centromere. *Science* **283**, 546–549 (1999).
37. Chen, B.-W., Lin, M.-H., Chu, C.-H., Hsu, C.-E. & Sun, Y.-J. Insights into ParB spreading from the complex structure of Spo0J and parS. *Proc. Natl. Acad. Sci. U.S.A.* **112**, 6613–6618 (2015).
38. Surtees, J. A. & Funnell, B. E. The DNA Binding Domains of P1 ParB and the Architecture of the P1 Plasmid Partition Complex. *J. Biol. Chem.* **276**, 12385–12394 (2001).
39. Ah-Seng, Y., Rech, J., Lane, D. & Bouet, J.-Y. Defining the role of ATP hydrolysis in mitotic segregation of bacterial plasmids. *PLoS Genet.* **9**, e1003956 (2013).
40. Fisher, G. L. *et al.* The structural basis for dynamic DNA binding and bridging interactions which condense the bacterial centromere. *Elife* **6**, (2017).
41. Madariaga-Marcos, J., Pastrana, C. L., Fisher, G. L., Dillingham, M. S. & Moreno-Herrero, F. ParB dynamics and the critical role of the CTD in DNA condensation unveiled by combined force-fluorescence measurements. *Elife* **8**, (2019).
42. Osorio-Valeriano, M. *et al.* ParB-type DNA Segregation Proteins Are CTP-Dependent Molecular Switches. *Cell* **179**, 1512-1524.e15 (2019).
43. Soh, Y.-M. *et al.* Self-organization of parS centromeres by the ParB CTP hydrolase. *Science* (2019) doi:10.1126/science.aay3965.
44. Easter, J. & Gober, J. W. ParB-Stimulated Nucleotide Exchange Regulates a Switch in Functionally Distinct ParA Activities. *Molecular Cell* **10**, 427–434 (2002).
45. Figge, R. M., Easter, J. & Gober, J. W. Productive interaction between the chromosome partitioning proteins, ParA and ParB, is required for the progression of the cell cycle in Caulobacter crescentus. *Mol. Microbiol.* **47**, 1225–1237 (2003).
46. Saenger, W., Orth, P., Kisker, C., Hillen, W. & Hinrichs, W. The Tetracycline Repressor—A Paradigm for a Biological Switch. *Angewandte Chemie International Edition* **39**, 2042–2052 (2000).
47. Onn, I. & Koshland, D. In vitro assembly of physiological cohesin/DNA complexes. *PNAS* **108**, 12198–12205 (2011).
48. Wu, L. J. & Errington, J. Coordination of cell division and chromosome segregation by a nucleoid occlusion protein in Bacillus subtilis. *Cell* **117**, 915–925 (2004).
49. Thanbichler, M. & Shapiro, L. MipZ, a Spatial Regulator Coordinating Chromosome Segregation with Cell Division in Caulobacter. *Cell* **126**, 147–162 (2006).

50. Kusiak, M., Gapczyńska, A., Płochocka, D., Thomas, C. M. & Jagura-Burdzy, G. Binding and Spreading of ParB on DNA Determine Its Biological Function in Pseudomonas aeruginosa. *J. Bacteriol.* **193**, 3342–3355 (2011).
51. Lin, D. C., Levin, P. A. & Grossman, A. D. Bipolar localization of a chromosome partition protein in Bacillus subtilis. *Proc. Natl. Acad. Sci. U.S.A.* **94**, 4721–4726 (1997).
52. Glaser, P. *et al.* Dynamic, mitotic-like behavior of a bacterial protein required for accurate chromosome partitioning. *Genes Dev.* **11**, 1160–1168 (1997).
53. Erdmann, N., Petroff, T. & Funnell, B. E. Intracellular localization of P1 ParB protein depends on ParA and parS. *Proc Natl Acad Sci U S A* **96**, 14905–14910 (1999).
54. Song, D., Rodrigues, K., Graham, T. G. W. & Loparo, J. J. A network of cis and trans interactions is required for ParB spreading. *Nucleic Acids Res.* **45**, 7106–7117 (2017).
55. Badrinarayanan, A., Le, T. B. K. & Laub, M. T. Rapid pairing and resegregation of distant homologous loci enables double-strand break repair in bacteria. *J Cell Biol* **210**, 385–400 (2015).
56. Jalal, A. S. B. *et al.* Evolving a new protein-DNA interface via sequential introduction of permissive and specificity-switching mutations. *bioRxiv* 724823 (2019) doi:10.1101/724823.

SUPPLEMENT TABLE S1. PLASMIDS, DNA, AND PROTEIN SEQUENCES

Plasmids/DNA	Description	Source
pET21b::*Caulobacter* ParB-His_6	Overexpression of C-terminally His_6-tagged *Caulobacter* ParB, carbenicillin^R >*Caulobacter* ParB-His_6 MSEGRRGLGRGLSALLGEVDAAPA**Q**^{35}APGEQLGGSREAPIEILQRNPDQ PRRTFREEDLEDLSNSIREKGVLQPILVRPSPDTAGEYQIVAGER**R**^{104}WRA AQRAGLKTVPIMVRELDDLAVLEIGIIENVQRADLNVLEEALSYKVLMEKF ERTQENIAQTIGKSRSHVANTMRLLALPDEVQSYLVSGELTAGHARAIAA AADPVALAKQIIEGGLSVRETEALARKAPNLSAGKSKGGRPPRVKDTDT QALESDLSSVLGLDVSIDHRGSTGTLTITYATLEQLDDL**C**^{297}NRLTRGIKLAA ALEHHHHHH* (numbering according to [1])	Gift from C. Jacob-Wagner [2]
pET21b::*Caulobacter* ParB-His_6 (C297S)	Overexpression of C-terminally His_6-tagged *Caulobacter* ParB (C297S), carbenicillin^R	This study
pET21b::*Caulobacter* ParB-His_6 (Q35C C297S)	Overexpression of C-terminally His_6-tagged *Caulobacter* ParB (Q35C C297S), carbenicillin^R	This study
pET21b::TetR-His_6	Overexpression of C-terminally His_6-tagged TetR (class B, from Tn10), carbenicillin^R >TetR (class B, from Tn10)-His_6 MSRLDKSKVINSALELLNEVGIEGLTTRKLAQKLGVEQPTLYWHVKNKRALL DALAIEMLDRHHTHFCPLEGESWQDFLRNNAKSFRCALLSHRDGAKVHL GTRPTEKQYETLENQLAFLCQQGFSLENALYALSAVGHFTLGCVLEDQEH QVAKEERETPTTDSMPPLLRQAIELFDHQGAEPAFLFGLELIICGLEKQLKC ESGSKLAAALEHHHHHH*	This study
pUC19::260bp-*parS*	pUC19 plasmid with 260-bp insert that contains *parS* sites, carbenicillin^R >260-bp_natural_*Caulobacter_parS*_fragment_cloned_into_pUC19 caagacgctcgcctcaatgcgaacgcccccgggttcgagcgggggcg ctggactcgatctatacgccaatcaggcgagcgggtcgatgtgactcatc ggcgtttcacgtgaaacacccccaccgcagctgtgagcggcctgtggac aatattggggatgttccacgtgaaacatcacttgccgatacagaaggtcg	This study

	aaaagacccgtccaagaacgtcctcaggatcgatacggccggagatg cgctccagggcccgggc	
pUC19::260bp-scrambled *parS*	pUC19 plasmid with 260-bp insert that contains scrambled *parS* sites, carbenicillin^{R} >260-bp_scrambled_*Caulobacter_parS*_fragment_cloned_into_pUC19 caagacgctcgcctcaatgcgaacgcccccgggttcgagcgggggcg ctggactcgatctatacgccaatcaggcgagcgggtcgatgtgactcatc ggacagctcgagattcatcccccaccgcagctgtgagcggcctgtggac aatattggggaatcgagtatacgctactcacttgccgatacagaaggtcg aaaagacccgtccaagaacgtcctcaggatcgatacggccggagatg cgctccagggcccgggc	This study
pET-His-MBP-TEV-DEST::*Sinorhizobium meliloti* ParB	For the purification of *Sinorhizobium meliloti* His_6-MBP-ParB	[3]
pET-His-MBP-TEV-DEST::*Rhodobacter sphaeroides* ParB	For the purification of *Rhodobacter sphaeroides* His_6-MBP-ParB	This study
pET-His-MBP-TEV-DEST::*Thermus thermophilus* ParB	For the purification of *Thermus thermophilus* His_6-MBP-ParB	[3]
pET-His-MBP-TEV-DEST::*Dechloromonas aromatica* ParB	For the purification of *Dechloromonas aromatica* His_6-MBP-ParB	This study
pET-His-MBP-TEV-DEST::*Psychrobacter* spp. ParB	For the purification of *Psychrobacter* spp. His_6-MBP-ParB	This study
pET-His-MBP-TEV-DEST::*Staphylococcus aureus* ParB	For the purification of *Staphylococcus aureus* His_6-MBP-ParB	[3]
pET-His-MBP-TEV-DEST::*Zymomonas mobilis* ParB	For the purification of *Zymomonas mobilis* His_6-MBP-ParB	This study
pET-His-MBP-TEV-DEST::*Xanthomonas campestris* ParB	For the purification of *Xanthomonas campestris* His_6-MBP-ParB	[3]
169bp_*parS*	cgccagggttttcccagtcacgacgttgtaaaacgacggccagtgaattcgagctcggtac ccgcaggaggacgtagggtaggggga**tgtttcacgtgaaaca**ggggatcctctagagtc gacctgcaggcatgcaagcttggcgtaatcatggtcatagctgtttcct	This study

169bp_scrambled_*parS*	cgccagggttttcccagtcacgacgttgtaaaacgacggccagtgaattcgagctcggtacc cgcaggaggacgtagggtaggggga***aattacactgagttta***ggggatcctctagagtcga cctgcaggcatgcaagcttggcgtaatcatggtcatagctgtttcct	This study
170bp_*parS*	cgccagggttttcccagtcacgacgttgtaaaacgacggccagaattcgcaacgtg **tgtttcacgtgaaaca**gccttgaactgataacgactctatcattgatagagtgttctct ccacgggatccccaggcatgcaagcttggcgtaatcatggtcatagctgtttcct	This study
around_pUC19_F	tcactcatggttatggcagcactgcataattc	This study
around_pUC19_F	taacactgcggccaacttacttctgacaacg	This study
20bp_*parS*_BLI_probeF	[Biotin]GGGAtgTTTCACGTGAAAca	This study
20bp_*parS*_BLI_probeR	tgTTTCACGTGAAAcaTCCC	This study
28bp_*tetO*_BLI_probeF	[Biotin]ggggactctatcattgatagagtatgc	This study
28bp_*tetO*_BLI_probeR	gcatactctatcaatgatagagtcccc	This study
20bp_*NBS*_BLI_probeF	[Biotin]GGGAtaTTTCCCGGGAAAta	This study
20bp_*NBS*_BLI_probeR	taTTTCCCGGGAAAtaTCCC	This study

Keys:
M13F (-47): cgccagggttttcccagtcacgac M13R: aggaaacagctatgaccat
parS: **tgtttcacgtgaaaca** scrambled *parS*: ***aattacactgagttta***
tetO: actctatcattgatagagt *Bam*HI RS: ggatcc *Eco*RI RS: gaattc

SUPPLEMENTARY REFERENCES

1. Tran, N. T. *et al.* Permissive zones for the centromere-binding protein ParB on the Caulobacter crescentus chromosome. *Nucleic Acids Res* **46**, 1196–1209 (2018).
2. Lim, H. C. *et al.* Evidence for a DNA-relay mechanism in ParABS-mediated chromosome segregation. *Elife* **3**, e02758 (2014).
3. Jalal, A. S. B. *et al.* Evolving a new protein-DNA interface via sequential introduction of permissive and specificity-switching mutations. *bioRxiv* 724823 (2019) doi:10.1101/724823.

FIG. 1

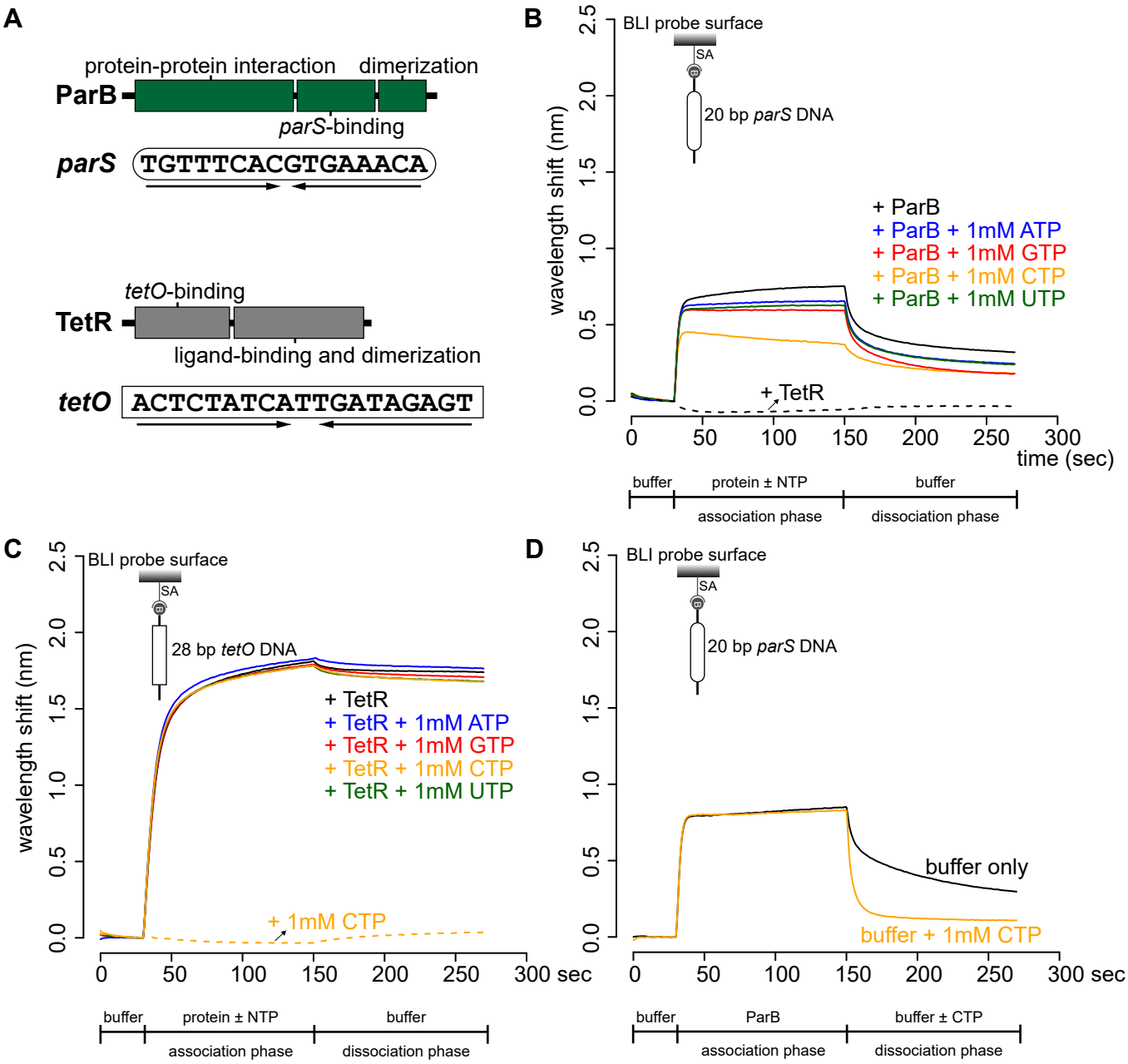

Figure 1. CTP reduces the nucleation of *Caulobacter* ParB at *parS*. (A) The domain architecture of ParB (dark green) and TetR (grey), and their respective DNA-binding sites *parS* and *tetO*. Convergent arrows below DNA-binding sites indicate that *parS* and *tetO* are palindromic. **(B)** Bio-layer interferometric (BLI) analysis of the interaction between a premix of 1 μM ParB-His_6 dimer ± 1 mM NTP and a 20-bp DNA duplex containing *parS*. Biotinylated DNA fragments were immobilized onto the surface of a Streptavidin (SA)-coated probe (See Materials and Methods). The BLI probe was dipped into a buffer only solution (0-30 sec), then to a premix of protein ± NTP (30-150 sec: association phase), and finally returned to a buffer only solution (150-270 sec: dissociation phase). Sensorgrams were recorded over time. BLI analysis of the interaction between 1 μM TetR-His_6 and a 20-bp *parS* probe was also recorded (a negative control). **(C)** BLI analysis of the interaction between a premix of 1 μM TetR-His_6 ± 1 mM NTP and a 28-bp DNA duplex containing *tetO*. BLI analysis of the interaction between 1 mM CTP and a 28-bp *tetO* probe was also recorded (a negative control). **(D)** BLI analysis of the interaction between 1 μM *Caulobacter* ParB-His_6 (without CTP) and a 20-bp *parS* DNA. For the dissociation phase, the probe was returned to a buffer only or buffer supplemented with 1 mM CTP. All buffers used for experiments in this figure contained Mg^{2+}. Each BLI experiment was triplicated and a representative sensorgram was presented.

FIG. 1-figure supplement 1

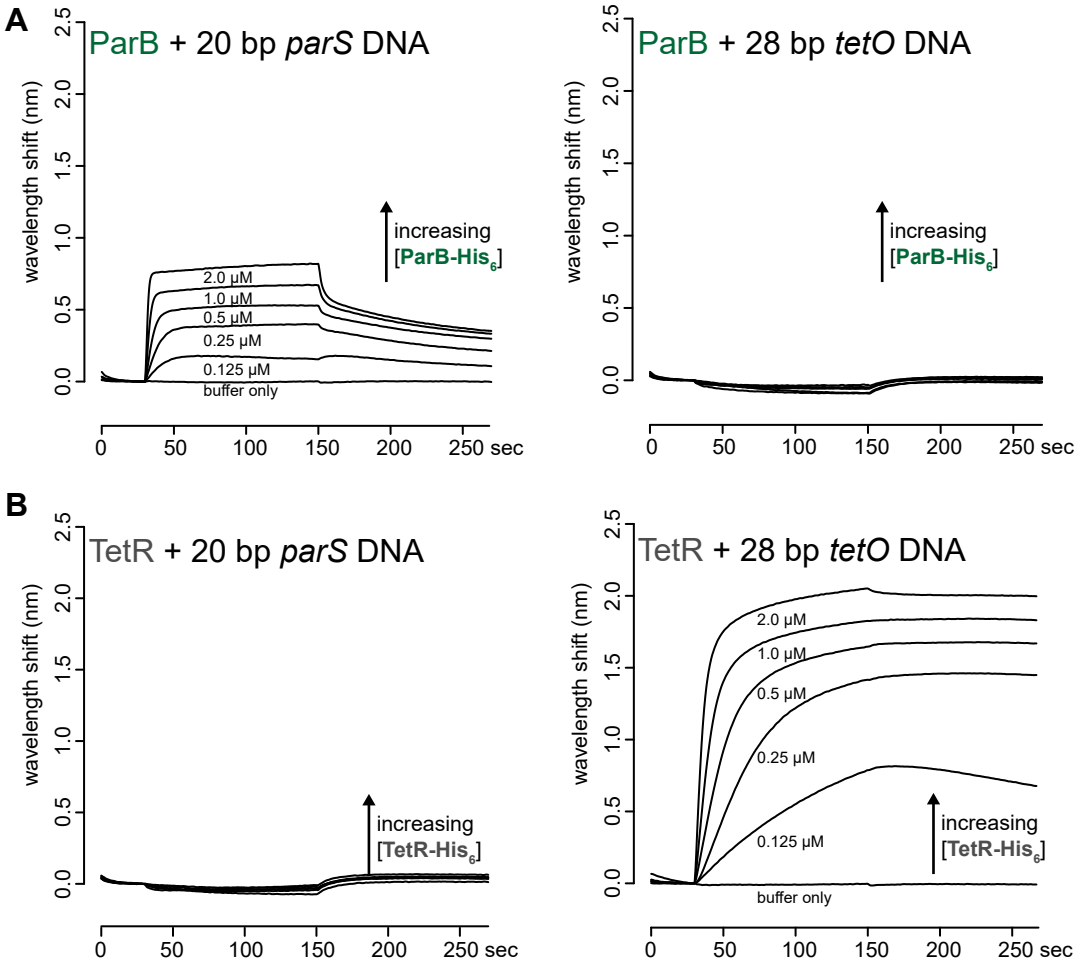

Figure 1-figure supplement 1. ParB and TetR bind specifically to their cognate binding sites *parS* and *tetO*, respectively. (A) BLI analysis of the interaction between purified *Caulobacter* ParB-His_6 (0.125 to 2 μM) and a 20-bp *parS* DNA probe or a 28-bp *tetO* DNA probe. **(B)** BLI analysis of the interaction between purified TetR-His_6 (0.125 to 2 μM) and a 20-bp *parS* DNA probe or a 28-bp *tetO* DNA probe.

FIG. 1-figure supplement 2

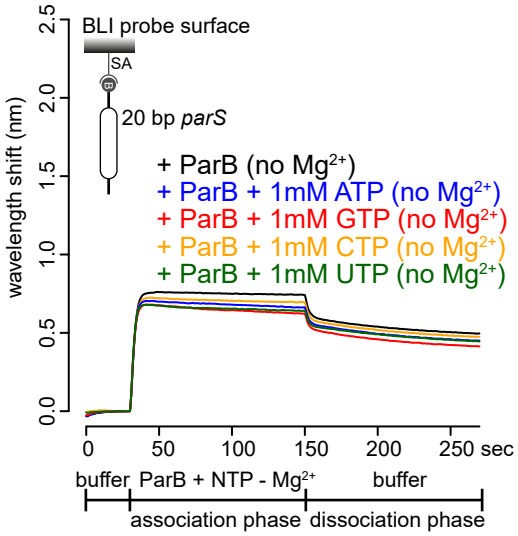

Figure 1-figure supplement 2. BLI analysis of the interaction between purified *Caulobacter* ParB and NTP in buffers lacking Mg^{2+}. *Caulobacter* ParB-His_6 (1 μM dimer) ± 1 mM NTP, and a 20-bp DNA duplex containing *parS* were used. Mg^{2+} was omitted from all buffers in this experiment. A schematic of the DNA substrate is shown above the sensorgram.

FIG. 1-figure supplement 3

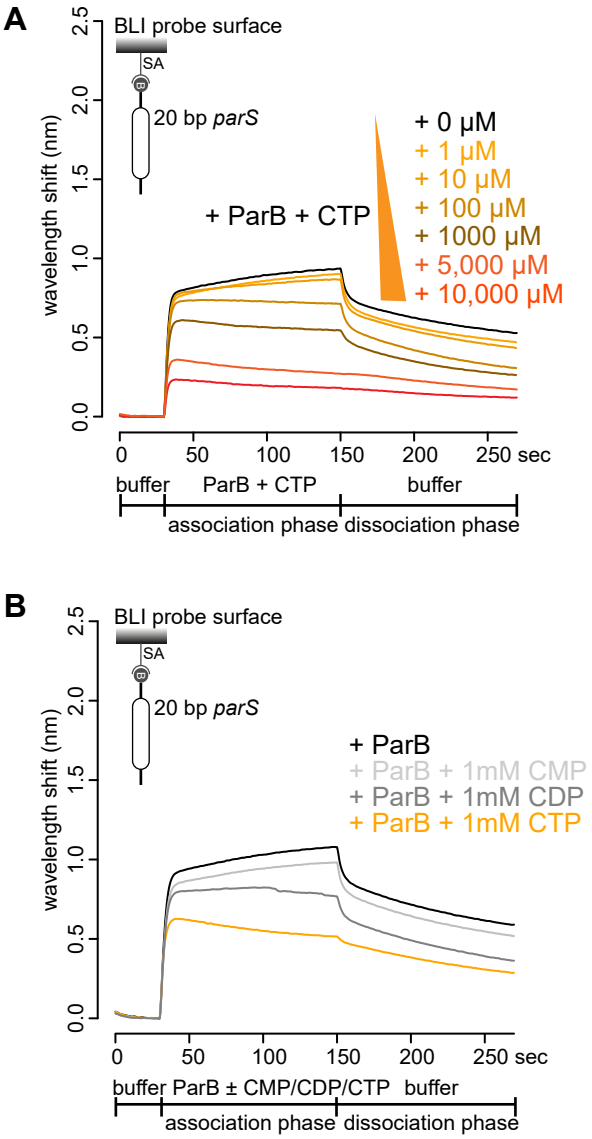

Figure 1-figure supplement 3. BLI analysis of the interaction between purified *Caulobacter* ParB and cytidine mono-, di-, or triphosphate. (A) BLI analysis of the interaction between purified *Caulobacter* ParB and an increasing concentration of CTP-Mg^{2+}. ParB-His_6 (1 µM dimer) + 0-10 mM CTP, and a 20-bp DNA duplex containing *parS* were used for this experiment. **(B)** BLI analysis of the interaction between a premix of 1 µM *Caulobacter* ParB-His_6 ± 1 mM cytidine mono-, di-, or triphosphate, and a 20-bp *parS* DNA. A schematic of the DNA substrate is shown above the sensorgram. Mg^{2+} was included in all buffers for experiments in this figure.

FIG. 2

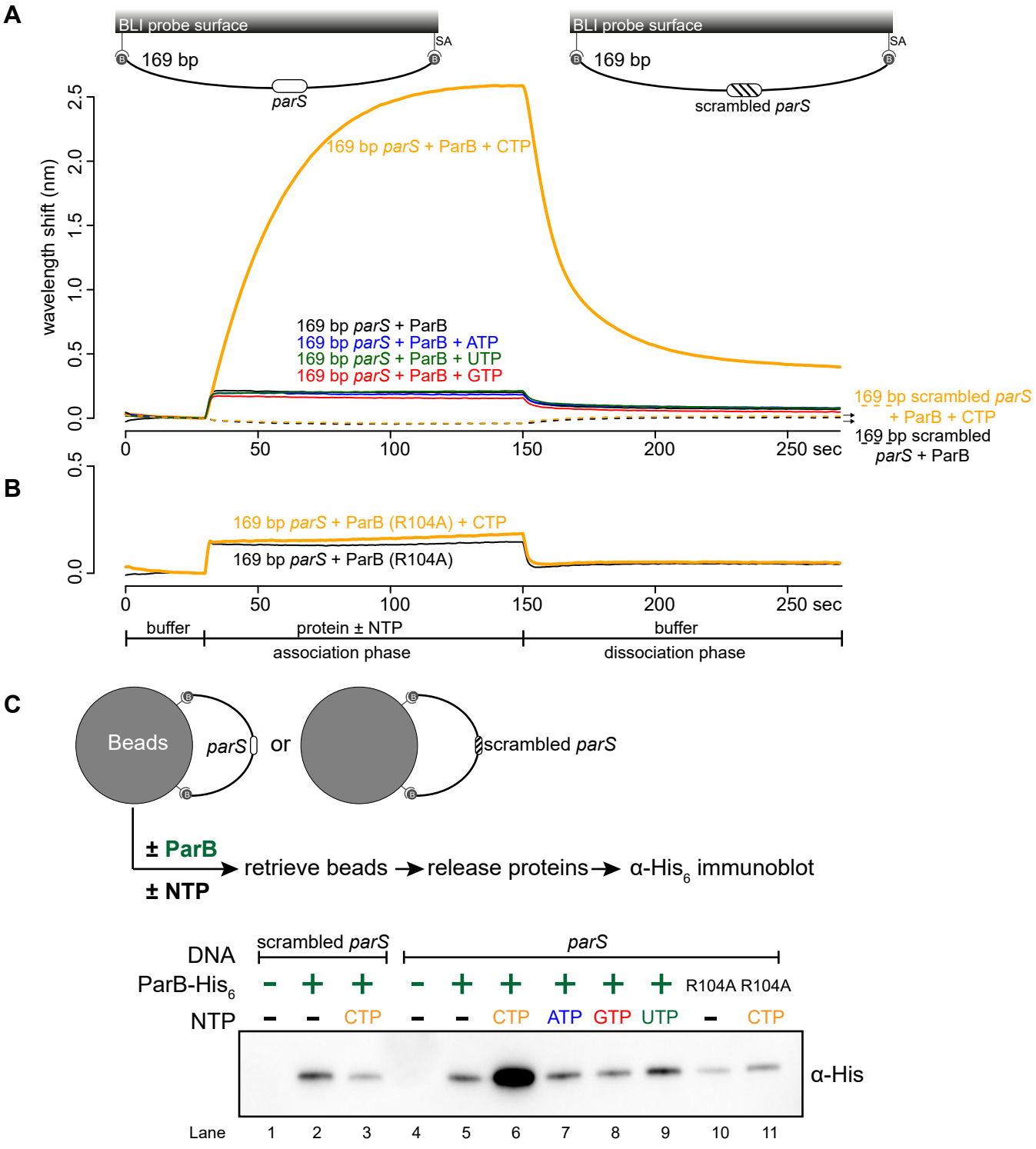

Figure 2. CTP facilitates ParB association with a closed DNA substrate beyond nucleation. (A) BLI analysis of the interaction between a premix of 1 μM *Caulobacter* ParB-His$_6$ ± 1 mM NTP and a 169-bp dual biotin-labeled DNA containing a *parS* or a scrambled *parS* site. Interactions between a dual biotinylated DNA and streptavidin (SA)-coated probe created a DNA substrate where both ends were blocked (a closed DNA substrate) (see the schematic of the BLI probes above the sensorgram). **(B)** Interactions between a nucleation-competent but spreading-defective ParB (R104) variant with a 169-bp *parS* DNA fragment in the presence or absence of CTP were also recorded. Each BLI experiment was triplicated and a representative sensorgram was presented. **(C)** A schematic of the pull-down assay and immunoblot analysis of pulled-down *Caulobacter* ParB-His$_6$. The length of bound DNA is ~2.8 kb. Beads were incubated with ParB protein for five minutes before being pulled down magnetically. All buffers used for experiments in this figure contained Mg^{2+}.

FIG. 2-figure supplement 1

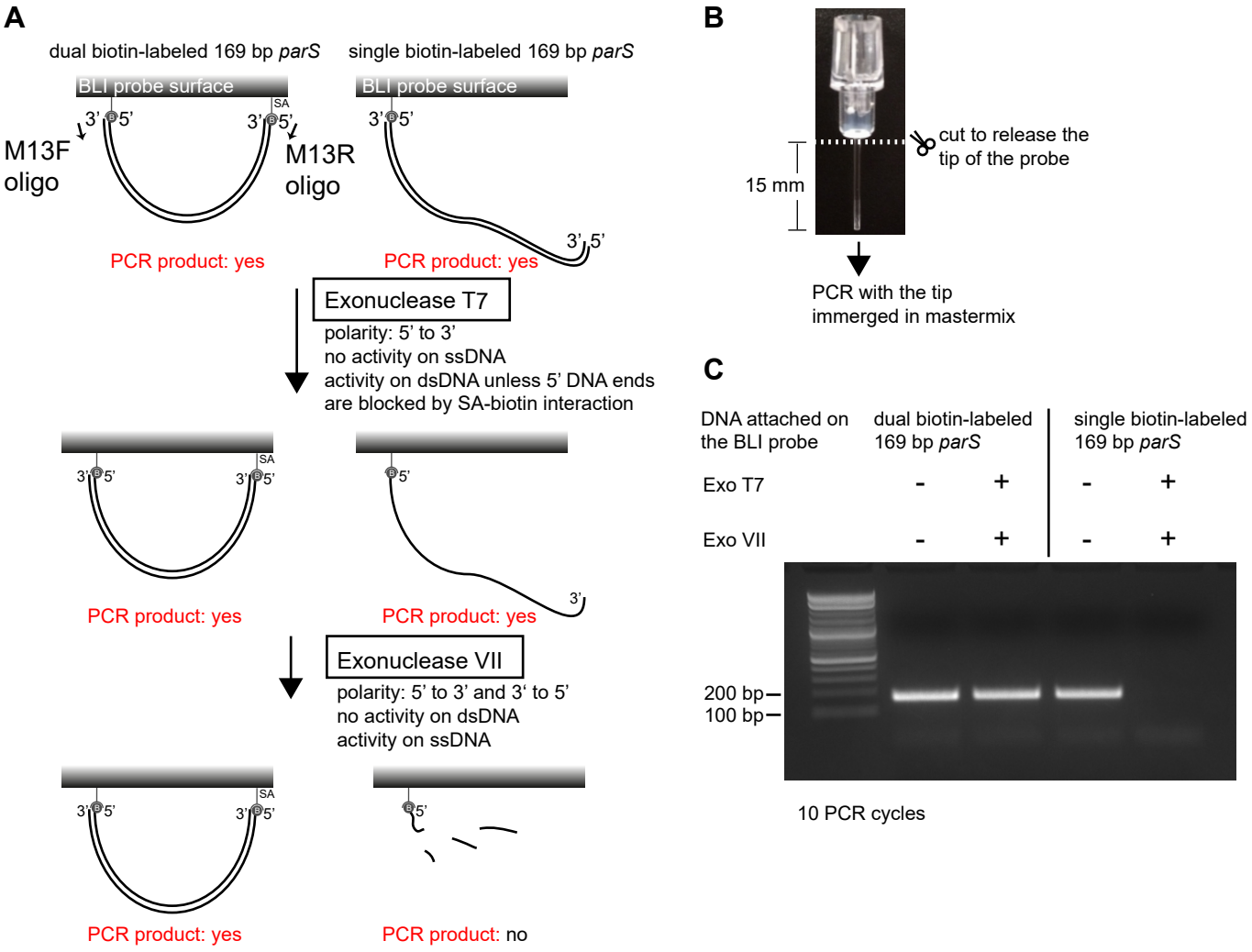

Figure 2-figure supplement 1. Dual biotin-labeled DNA fragments form a closed substrate on the surface of the BLI probe. (A) A schematic of a double digestion assay using Exonuclease T7 + Exonuclease VII and PCR. PCR was performed using M13F, M13R oligos, and DNA attached to the BLI surface as a template. **(B)** The BLI probe was severed from the plastic adaptor and immerged into a PCR master mix. **(C)** Dual biotin-labeled DNA fragments on the BLI surface were resistant to Exo T7 + Exo VII digestion while single biotin-labeled DNA fragments on the BLI surface were not.

FIG. 2-figure supplement 2

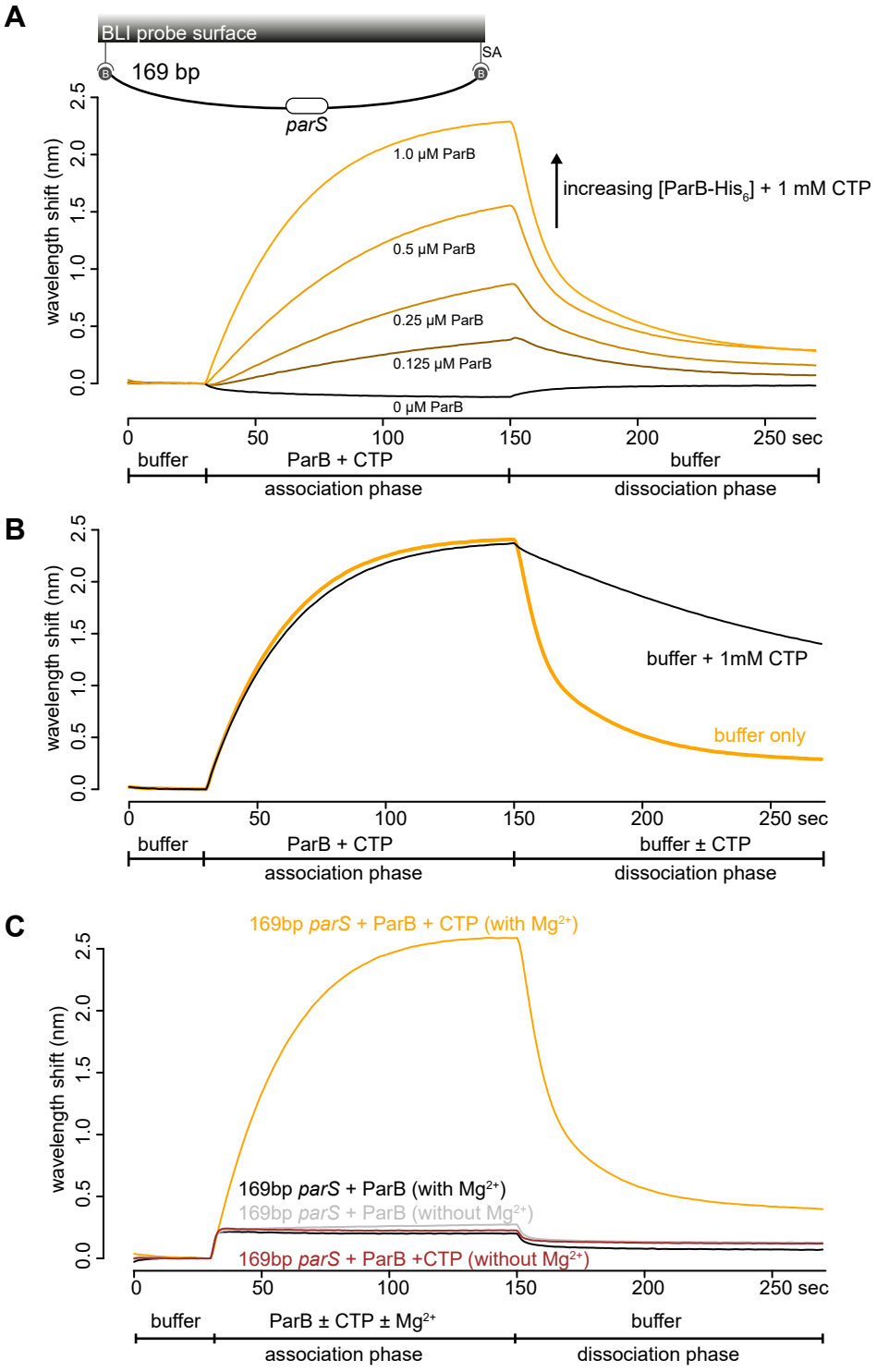

Figure 2-figure supplement 2. CTP-Mg^{2+} enhances ParB accumulation on a closed DNA substrate. (A) BLI analysis of the interaction between an increasing concentration of *Caulobacter* ParB-His_6 (0.125 to 1.0 µM) + 1 mM CTP and a 169-bp dual biotin-labeled *parS* DNA. A schematic of the DNA substrate is shown above the sensorgram. **(B)** BLI analysis of the interaction between 1 µM *Caulobacter* ParB-His_6 (with 1 mM CTP) and a 169-bp dual biotin-labeled *parS* DNA. For the dissociation phase, the probe was returned to a buffer only or buffer supplemented with 1 mM CTP solution. All buffers used for experiments in panel A-B contained Mg^{2+}. **(C)** BLI analysis of the interaction between a premix of 1 µM *Caulobacter* ParB-His_6 ± 1 mM CTP and a 169-bp dual biotin-labeled DNA containing a *parS* site in buffer with or without $MgCl_2$.

FIG. 2-figure supplement 3

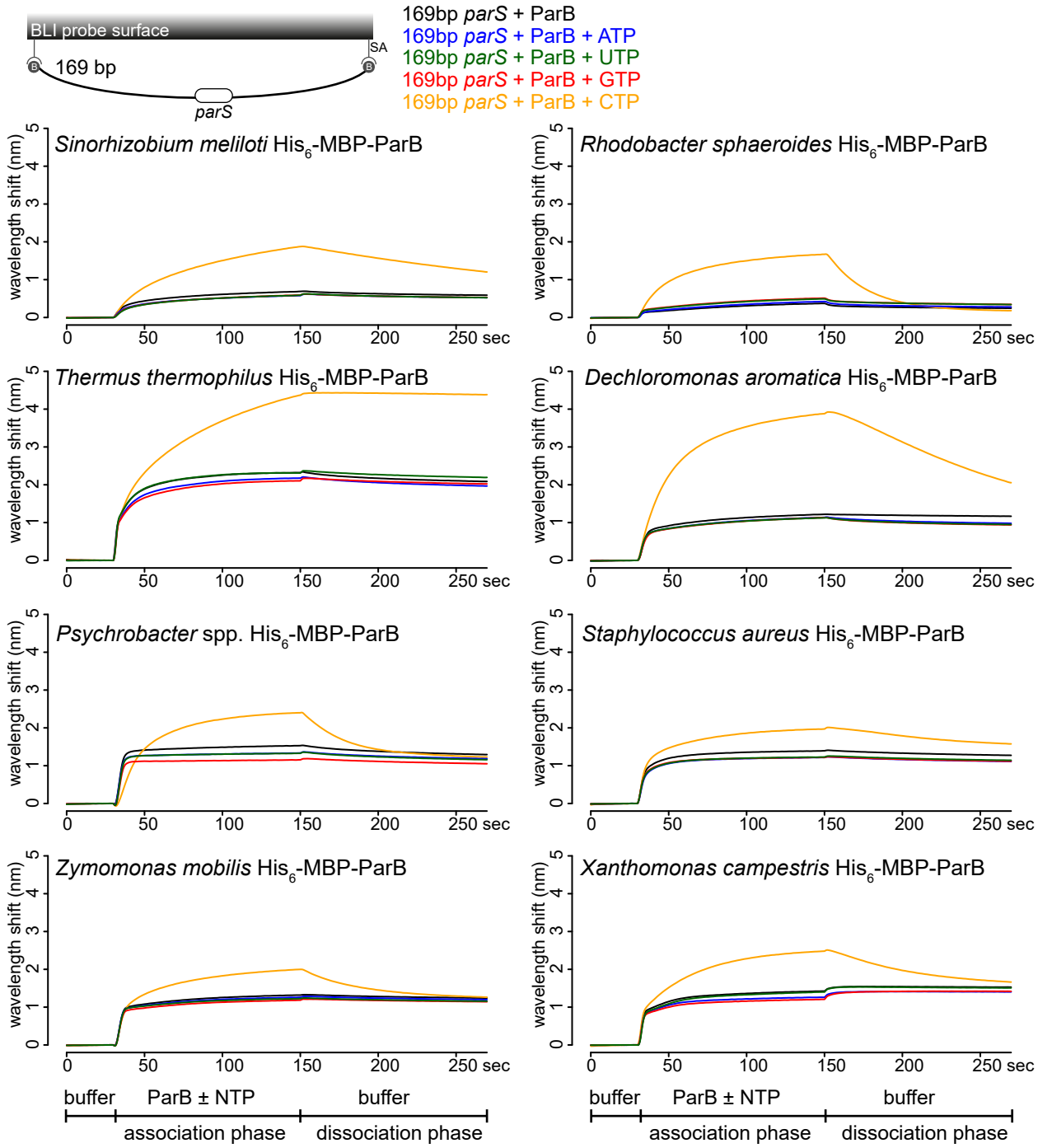

Figure 2-figure supplement 3. CTP facilitates the association of eight ParB orthologs with DNA. BLI analysis of the interaction between a premix of 1 μM His_6-MBP-tagged ParB proteins from a set of diverse bacterial species ± NTPs and a 169-bp dual biotin-labeled *parS* DNA. NTPs at 1 mM (final concentration) was used, except for BLI experiments with *Zymomonas mobilis* and *Xanthomonas campestris* ParBs where 0.01 mM CTP was used instead. Mg^{2+} was included in all buffers for this experiment. A schematic of the DNA substrate is shown above the sensorgrams.

FIG. 3

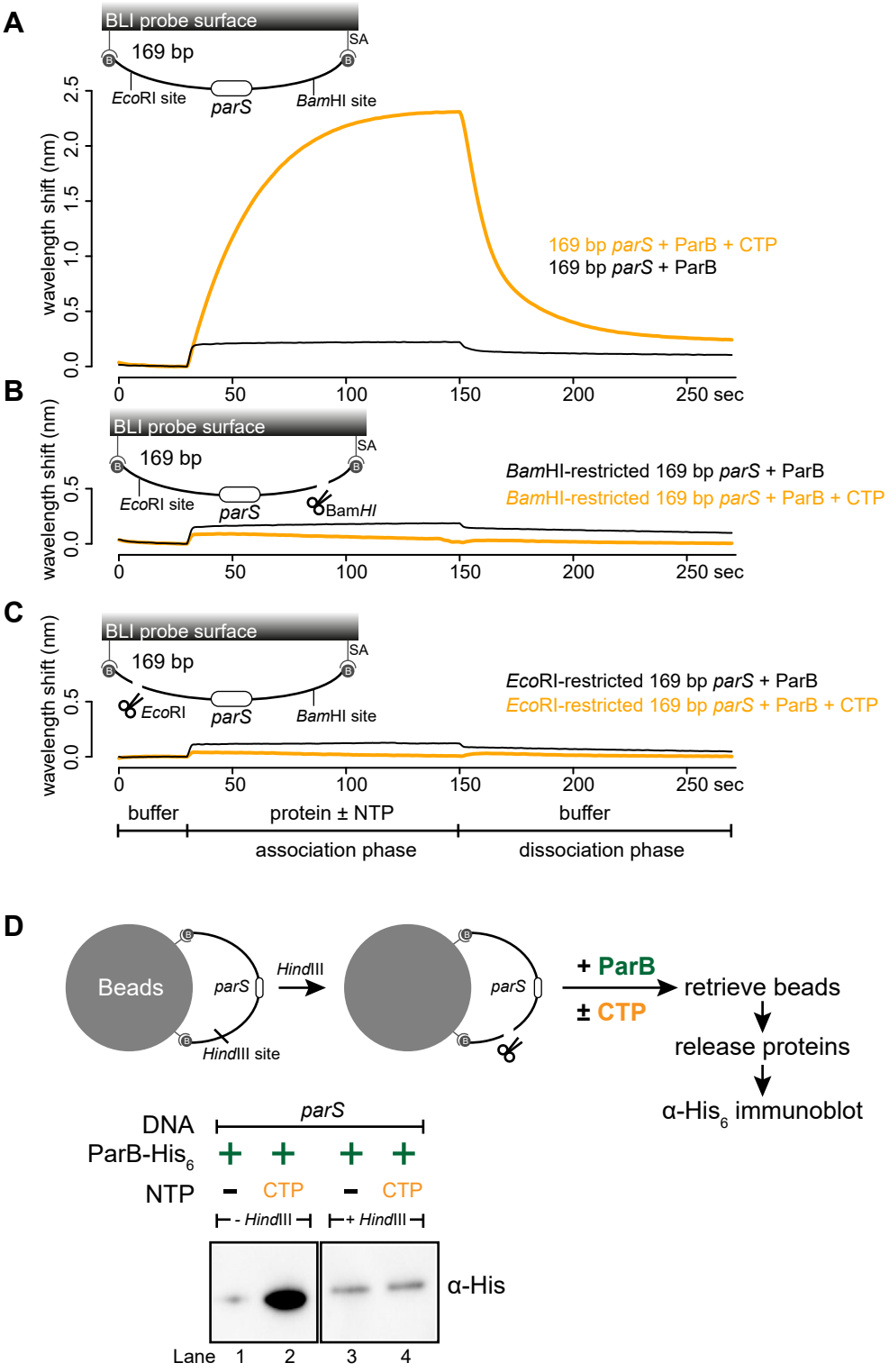

Figure 3. A closed DNA substrate is required for an increased association of ParB with DNA. (A) BLI analysis of the interaction between a premix of 1 µM *Caulobacter* ParB-His$_6$ ± 1mM CTP and a 169-bp dual biotin-labeled *parS* DNA. **(B)** Same as panel A but immobilized DNA fragments have been restricted with *Bam*HI before BLI analysis. **(C)** Same as panel A but immobilized DNA fragments have been restricted with *Eco*RI before BLI analysis. Schematic of DNA fragments with the relative positions of *parS* and restriction enzyme recognition sites are shown above the sensorgram. Each BLI experiment was triplicated and a representative sensorgram was presented. **(D)** A schematic of the pull-down assay and immunoblot analysis of pulled-down *Caulobacter* ParB-His$_6$. For lanes 3 and 4, DNA-bound beads were incubated with *Hind*III to linearize bound DNA. Samples in lanes 1-4 were loaded on the same gel, the immunoblot was spliced together for presentation purposes. All buffers used for experiments in this figure contained Mg^{2+}.

FIG. 3-figure supplement 1

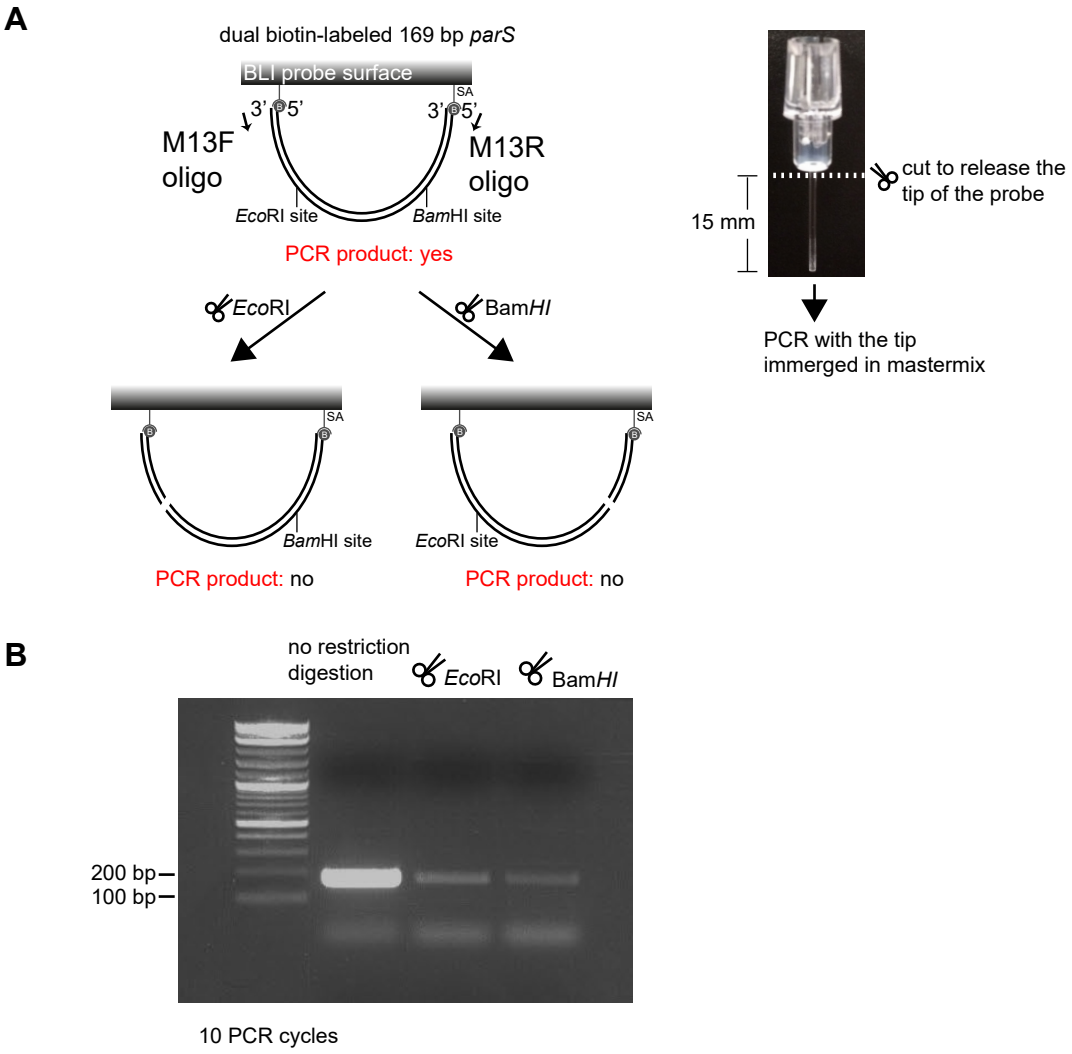

Figure 3-figure supplement 1. Restriction enzymes linearize dual biotin-labeled DNA fragments on the surface of the BLI probe. (A) (Left panel) A schematic of a digestion assay using *Bam*HI/*Eco*RI and PCR. PCR was performed using M13F, M13R oligos, and DNA attached to the BLI surface as a template. **(Right panel)** The BLI probe was severed from the plastic adaptor and immerged into a PCR master mix. **(B)** Detection of intact 169-bp DNA fragments that were bound on the surface of the BLI probe before and after treatment with restriction enzymes.

FIG. 3-figure supplement 2

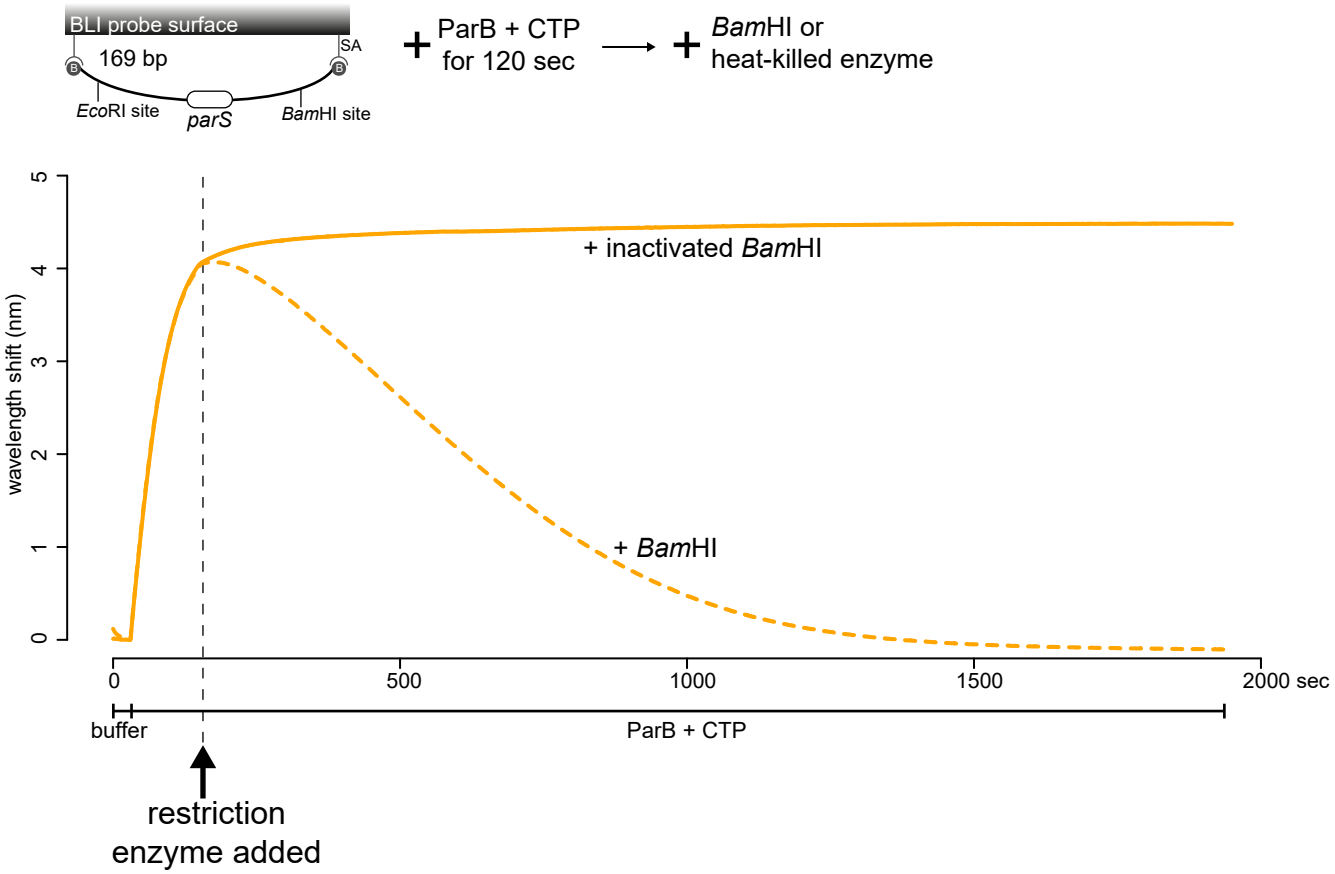

Figure 3-figure supplement 2. Linearization of a closed DNA substrate by *Bam*HI liberates pre-bound ParB from DNA. *Bam*HI was added after 1 μM *Caulobacter* ParB-His$_6$ + 1mM CTP and a 169-bp dual biotin-labeled *parS* DNA were preincubated together for 120 sec. As a negative control, heat-inactivated *Bam*HI was added instead. Mg^{2+} was included in all buffers for this experiment. A schematic of the DNA substrate is shown above the sensorgram.

FIG. 4

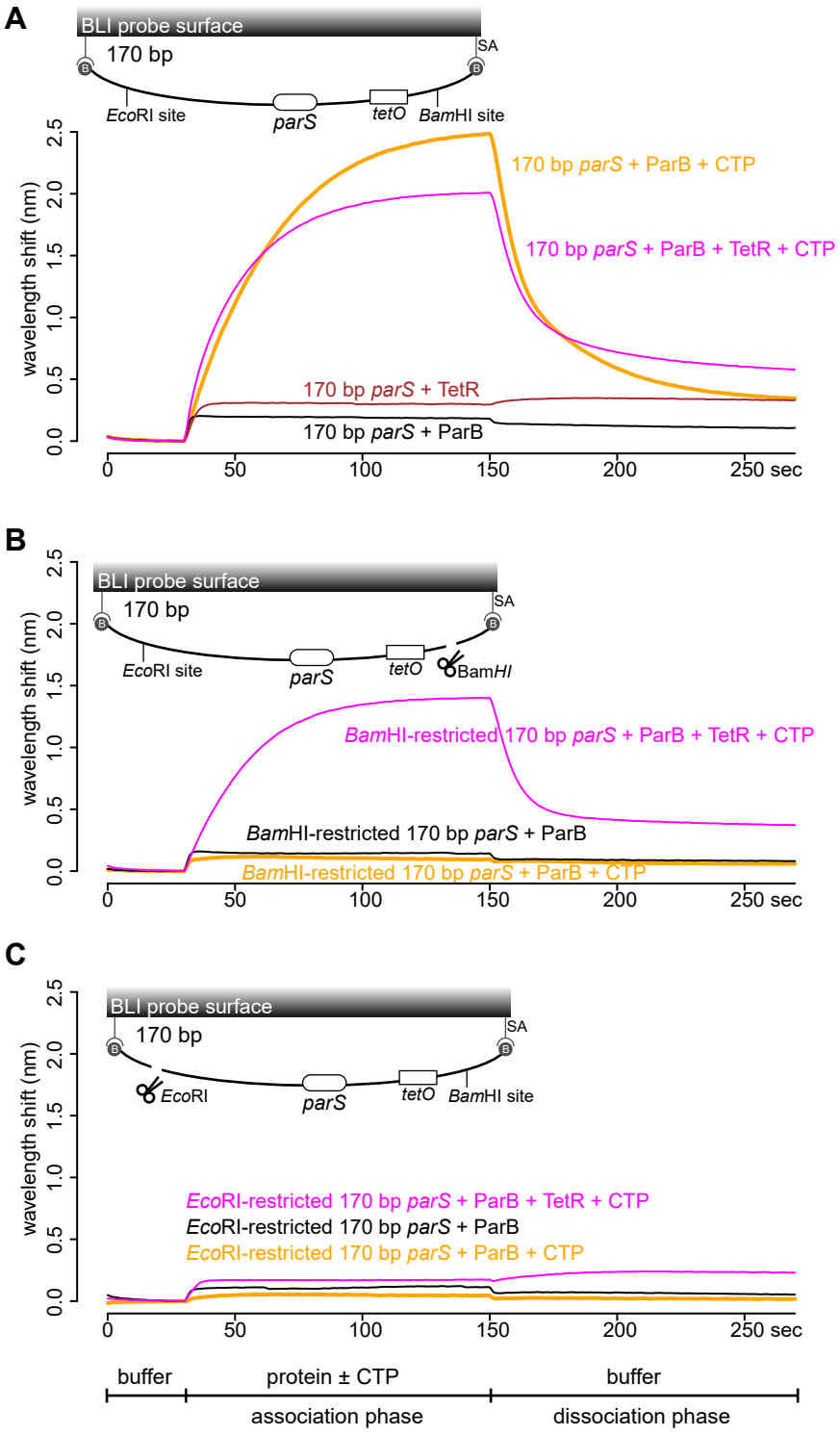

Figure 4. TetR-*tetO* binding restores ParB association with an opened DNA substrate. (A) BLI analysis of the interaction between a premix of 1 μM *Caulobacter* ParB-His$_6$ ± 1mM CTP ± 1 μM TetR-His$_6$ and a 170-bp dual biotin-labeled DNA containing a *parS* site. **(B)** Same as panel A but immobilized DNA fragments have been restricted with *Bam*HI before BLI analysis. **(C)** Same as panel A but immobilized DNA fragments have been restricted with *Eco*RI before BLI analysis. Schematic of DNA fragments together with the relative positions of *parS*, *tetO*, and restriction enzyme recognition sites are shown above the sensorgram. Each BLI experiment was triplicated and a representative sensorgram was presented. All buffers used for experiments in this figure contained Mg^{2+}.

FIG. 4-figure supplement 1

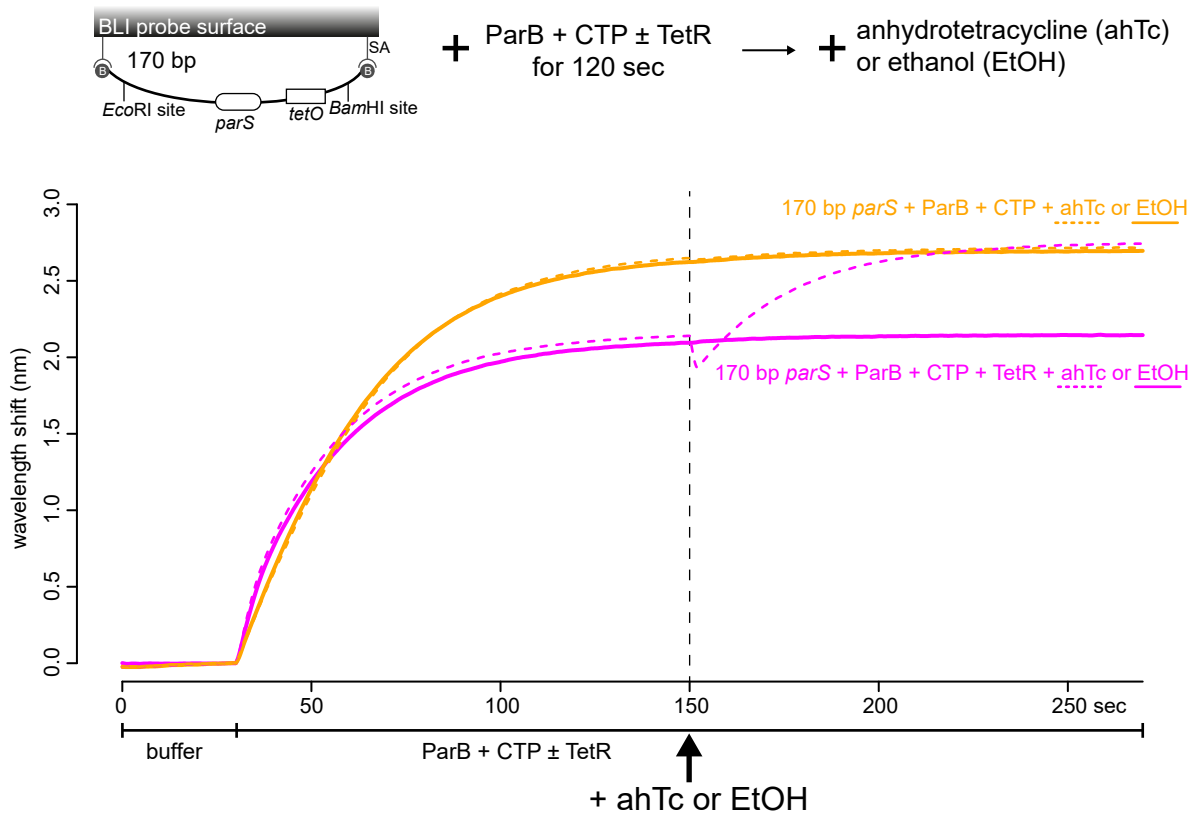

Figure 4-figure supplement 1. Anhydrotetracycline removes DNA-bound TetR roadblock and allows ParB to accumulate further on DNA. Anhydrotetracycline (3 μM) or ethanol (0.01%) was added after 1 μM *Caulobacter* ParB-His_6 + 1mM CTP ± 1 μM TetR and a 170-bp dual biotin-labeled *parS* DNA were preincubated together for 120 sec. Mg^{2+} was included in all buffers for this experiment. A schematic of the DNA substrate is shown above the sensorgram.

FIG. 5

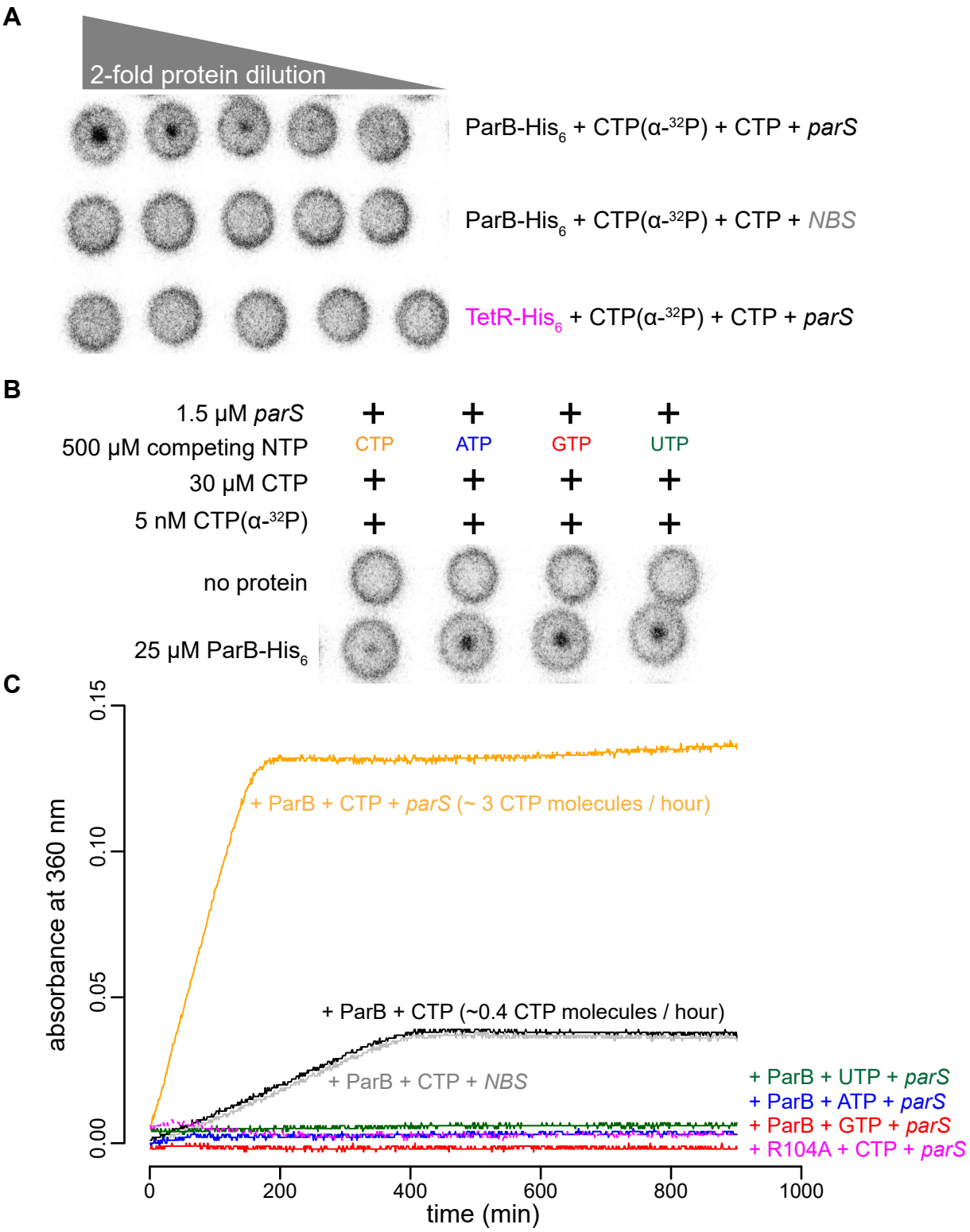

Figure 5. *parS* DNA increases the CTP binding and hydrolysis rate by *Caulobacter* ParB. (A-B) CTP binding as monitored by DRaCALA assay using radiolabeled CTP α-P^{32}. The bulls-eye staining indicates CTP binding due to a more rapid immobilization of protein-ligand complexes compared to free ligands alone. The starting concentration of proteins used in panel A was 25 μM. The same concentration of radioactive CTP, unlabeled CTP, and DNA was used in experiments shown in panels A and B. **(C)** A continuous monitoring of inorganic phosphate (Pi) released by recording absorbance at 360 nm overtime at 25°C. The rates of CTP hydrolysis were inferred from a Pi standard. The NTP hydrolysis of *Caulobacter* ParB was also monitored in the presence of ATP, GTP, or UTP, with a 22-bp *parS* DNA duplex or a non-cognate 22-bp *NBS* DNA duplex (a DNA-binding site of Noc protein (Wu and Errington, 2004)). The nucleation-competent but spreading-defective ParB (R104A) mutant did not hydrolyze CTP in the presence of *parS* DNA. All buffers used for experiments in this figure contained Mg^{2+}.

FIG. 6

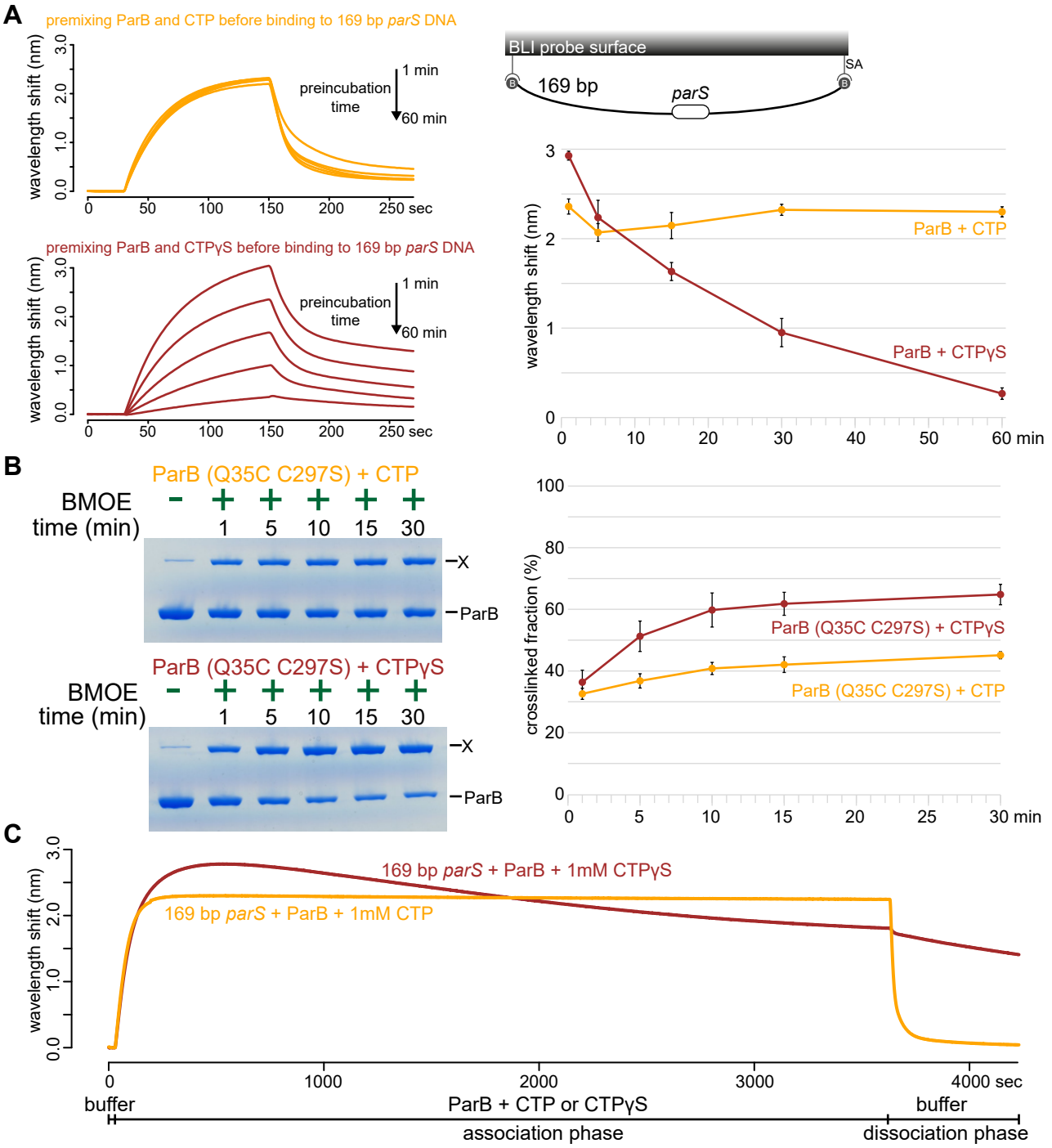

Figure 6. ParB accumulation on DNA is unstable in the presence of a non-hydrolyzable analog CTPγS. (A) (Left panel) BLI analysis of the interaction between a premix of 1 μM *Caulobacter* ParB-His_6 ± 1mM CTP or CTPγS and a 169-bp dual biotin-labeled *parS* DNA. Purified ParB was preincubated with CTP or CTPγS for 1, 5, 15, 30, or 60 min before BLI analysis. **(Right panel)** Quantification of ParB-DNA interaction at the end of each association phase (150^{th} sec). Error bars represent SD from three replicates. **(B) (Left panel)** Time course of *Caulobacter* ParB (Q35C C297S) cross-linking with CTP or CTPγS in the absence of *parS* DNA. Purified ParB-His_6 (Q35C C297S) (10 μM) were preincubated with 1 mM CTP or CTPγS for 1, 5, 10, 15, or 30 min before BMOE was added. X indicates a cross-linked form of ParB. **(Right panel)** Quantification of the cross-linked (X) fractions. Error bars represent SD from three replicates. **(C)** BLI analysis of the interaction between a premix of 1 μM *Caulobacter* ParB-His_6 ± 1mM CTP or CTPγS and a 169-bp dual biotin-labeled *parS* DNA. CTP or CTPγS was added to purified ParB, and the mixture was immediately used for BLI experiments. All buffers used for experiments in this figure contained Mg^{2+}.

FIG. 6-figure supplement 1

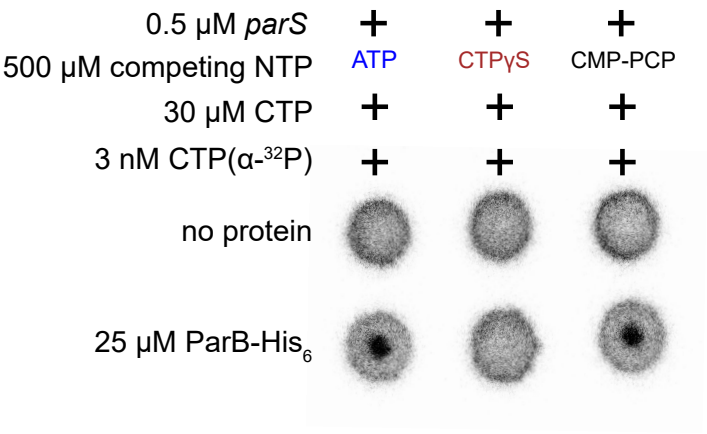

Figure 6-figure supplement 1. *Caulobacter* ParB binds CTP and a non-hydrolyzable analog CTPγS but not CMP-PCP. CTPγS (but not CMP-PCP) outcompeted radioactive CTP α-P^{32} for binding to ParB-*parS* complex, indicating that *Caulobacter* ParB can bind to CTPγS. Binding to radioactive CTP α-P^{32} was monitored by DRaCALA assay. The bulls-eye staining indicates CTP binding due to a more rapid immobilization of protein-ligand complexes compared to free ligands alone.

FIG. 6-figure supplement 2

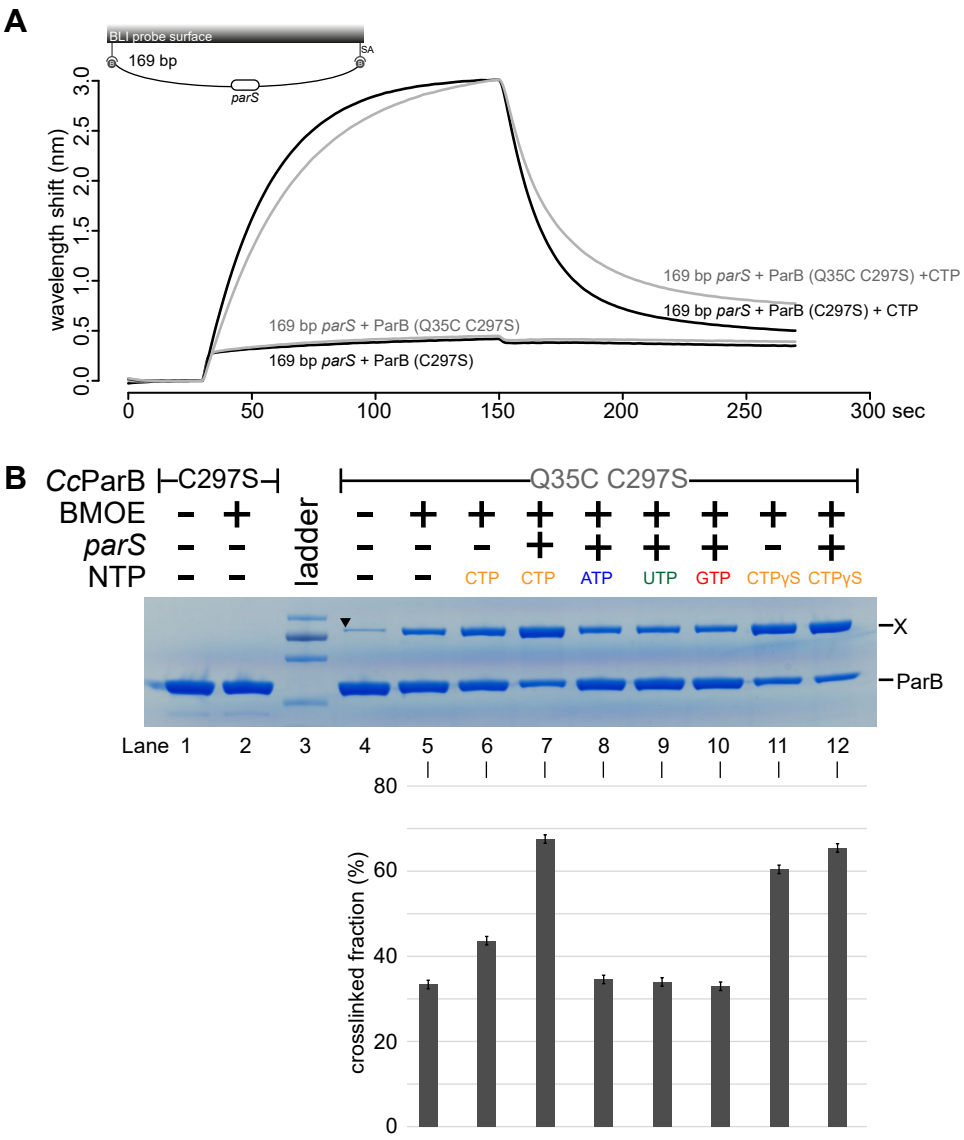

Figure 6-figure supplement 2. BLI analysis and gel analysis of cross-linking products of purified *Caulobacter* ParB (Q35C C297S). (A) BLI analysis of the interaction between a premix of 1 µM His-tagged ParB (C97S) or (Q35C C297S) ± 1mM CTP and a 169-bp dual biotin-labeled *parS* DNA. In the presence of CTP, both variants of ParB were able to spread, indicating that the engineered mutations Q35C and C297S did not impair the function of ParB *in vitro*. **(B)** Purified *Caulobacter* ParB-His_6 (Q35C C297S) ± NTPs ± *parS* DNA were incubated for 15 min at room temperature before cross-linking with BMOE. A cysteine-less ParB (C297S) was used as a negative control. X indicates a cross-linked form of ParB. A solid black triangle on lane 4 indicates a contaminated protein from the purification of ParB-His_6 (Q35C C297S). A lower panel shows the quantification of the cross-linked (X) fractions. Error bars represent SD from three replicates.

FIG. 7

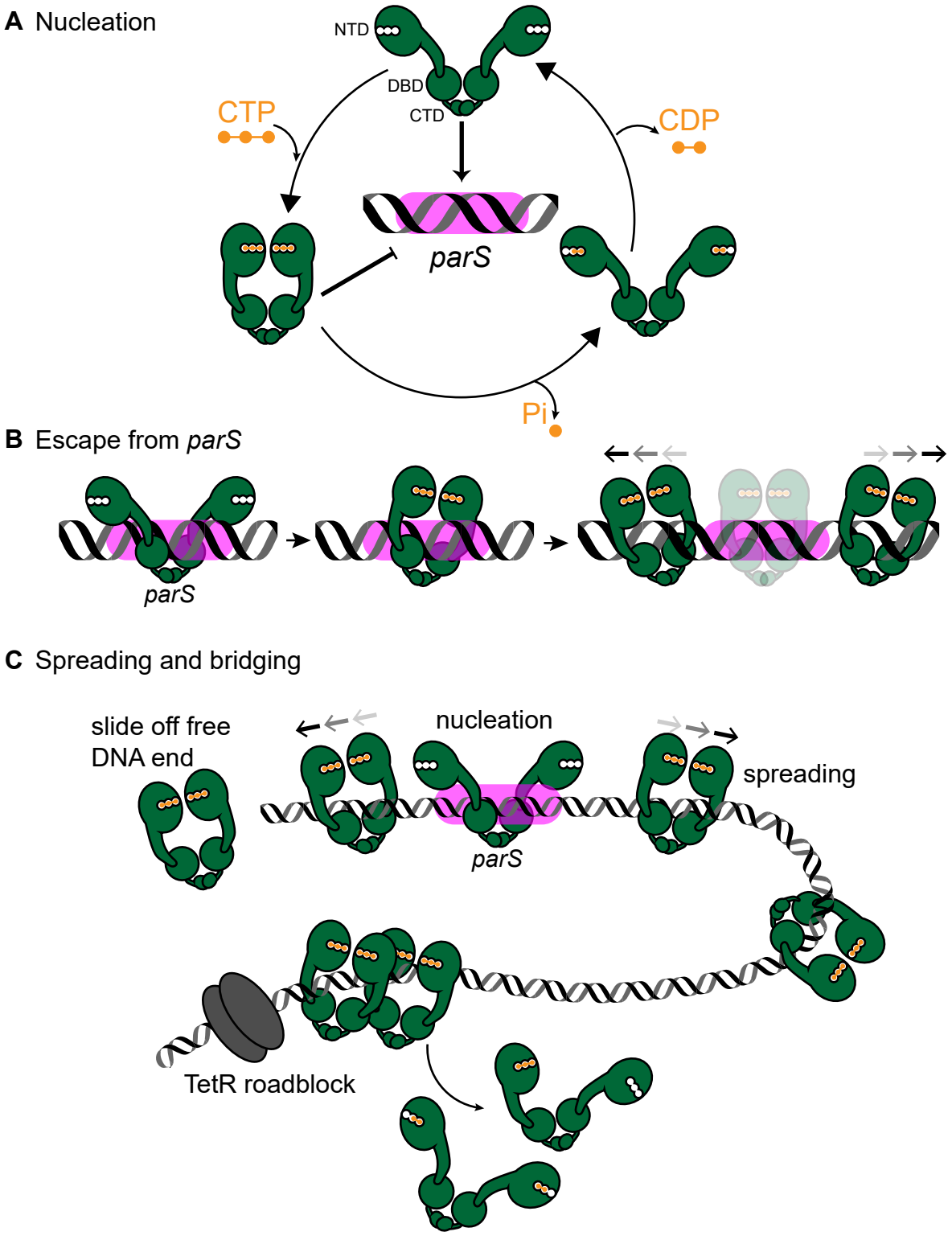

Figure 7. A model for *Caulobacter* ParB nucleation and spreading. (A) *Caulobacter* ParB nucleation at *parS*. CTP (orange) reduces *Caulobacter* ParB (dark green) nucleation at *parS* (magenta box), presumably by inducing conformational changes that are incompatible with a site-specific *parS* binding (Soh et al., 2019). Only apo- or CDP-bound ParB can nucleate on *parS*. ParB hydrolyzes CTP at a faster rate in the presence of *parS*. The domain architecture of ParB is also shown: NTD: N-terminal domain, DBD: DNA-binding domain, and CTD: C-terminal domain. **(B)** *Caulobacter* ParB escapes from the nucleation site *parS*. Apo-ParB at *parS* binds CTP and slides laterally away from the nucleation site *parS* while still associating with DNA. **(C)** *Caulobacter* ParB sliding and spreading on DNA. CTP-bound ParBs diffuse from the nucleation site *parS* and can run off the free DNA end unless they are blocked by DNA-bound roadblocks such as transcriptional regulators e.g. TetR. CTP hydrolysis is not required for ParB to escape from the nucleation *parS* site but might contribute to ParB recycling. It is not yet known whether both CTP molecules on a ParB dimer are concertedly hydrolyzed/dissociated for ParB to escape from the chromosome or a heterodimer state of ParB with a single CTP bound also exists *in vivo*.